SSD ING IND04 Costruzioni e Strutture Aerospaziali

Paolo Gaudenzi, Paolo Gasbarri, Franco Mastroddi, Giuliano Coppotelli, Claudio Scarponi, Luca Lampani

SAPIENZA
UNIVERSITÀ DI ROMA

Febbraio, 2017

People (and papers)






Journals

Composite structures (4)
Acta astronautica (7)
Composites part B (5)
Intelligent material systems and structures (2)
Meccanica (1)
Materials and design (1)
Journal of sound and vibration (1)
Journal of fluid and structures (1)
Mechanical systems and signal processing (1)
Advances in space research (1)
Advances in the astronautical sciences (3)
Journal of aircraft (1)
Experimental techniques (1)

27 papers (2015-17)

Labs

Lab Name: Aerospace Composite Structures (heavy)
Facilities: Autoclave for thermosetting curing of composites, and relevant subsiadiary equipments (including ultrasonic inspection device)
Activities: Constructuion of structural components in composite materials (active composites, natural fibers composites, aeronautical elements)
Lab Name: Structural Dynamics lab (heavy)
Facilities: Vibration table for structural dynamic tests and relevant equipments and control electronics
Activities: Experimental studies

Lab Name: Fluid-structure interaction and aeroelasticity computational lab
Facilities: Cluster of workstations equipped with in-house software and commercial packages
Activities: Computational models for fluid-structure interaction, MDO analysis, verification and design

Lab Name: Multybody dunamics computational lab
Facilities: Cluster of workstations equipped with in-house software and commercial packages
Activities: Computational models for multybody dynamics simulations and for design of robotic experiments

Labs

Lab Name: Smart Structures lab
Facilities: Light electronic equipment for the construction and testing of smart structurre components
Activities: Experimental testing and harware development of active structures (with embedded piezoelectric actuators/sensors) or electronics

Lab Name: Concurrent design lab for space systems
Facilities: Cluster of workstation for satellite system design
Activities: Design of space mission and systems (phase A)

Lab Name: Ground station for UHF/VHF link with space systems
Facilities: Antenna able to follow LEO missions and relevant UHF/VHF radio equipment
Activities: Educational activities for the students of master in satellites

List of Projects

Title Smart Composite Structures	
Participants: P. Gaudenzi, L. Lampani, C. Scarponi M. Pasquali (AR),	
Period: insert period	**Sponsor**: insert sponsor

Title Space systems design	
Participants: P. Gaudenzi G. Palermo (PHD 3^ year), L. Pollice (PHD 2^ year)	
Period: insert period	**Sponsor**: insert sponsor

Title Structural design and analysis for additive manufacturing	
Participants: P. Gaudenzi M. Eugeni (AR), V. Cardini (PHD 1^ year), H. Elihai (PHD 1^year)	
Period: insert period	**Sponsor**: insert sponsor

Advanced/active composites

P. Gaudenzi, L. Lampani

Wireless smart composite structures

- Manufacturing techniques for embedding electronics and active elements (piezo, SMA) in a thermoset carbon fibers or glass fibers composites
- Implementation of embedded energy harvesting devices (SSS)
- Implementation of attached/embedded wireless transmission for structural sensing (SSS)

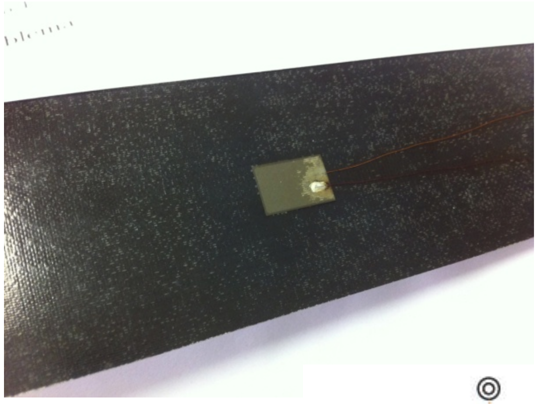

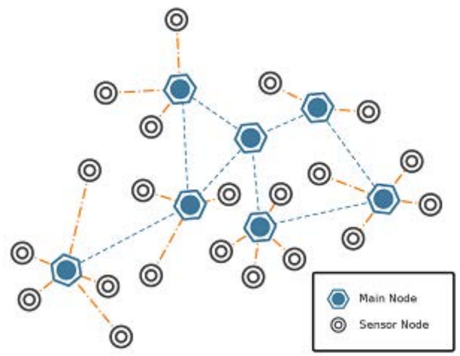

Advanced/active composites

P. Gaudenzi, L. Lampani

- Design and manufacturing of advanced small sat (e.g. cubesat) composite structures
- Design and manufacturing of electronic box of space payloads or subsystem components in composite structures
- Sapienza flight team airplane (models) structures
- Embedded space flight electronic hardware (e.g. On-board data handling subsystem) in composite structural panels offering multiple functionality and versatility in spacecraft configuration (TASI)

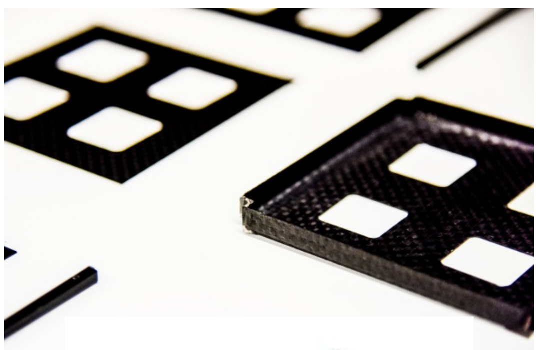

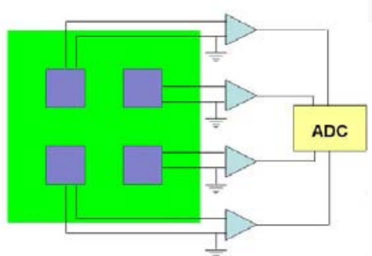

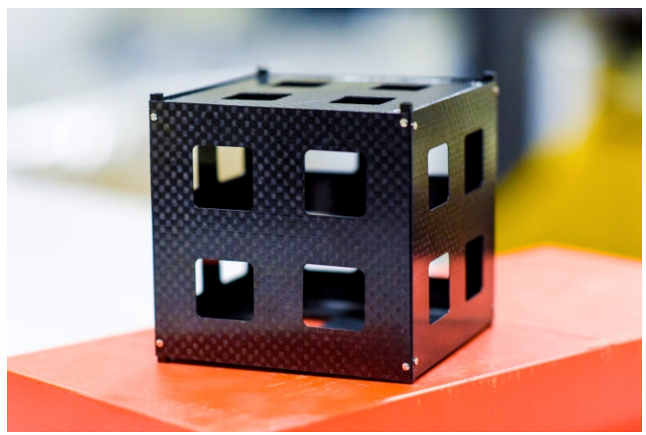

High velocity impact (HVI) on composite structures

P. Gaudenzi, L. Lampani

1. ***Experimental campaign on CFRPs woven laminated plates*** in cooperation with:

- **Department of Chemical Engineering Materials Environment, University La Sapienza, Rome**
  Prof. Teodoro Valente

➢ Realization and mechanical characterization of CFRP specimens

Vacuum bag

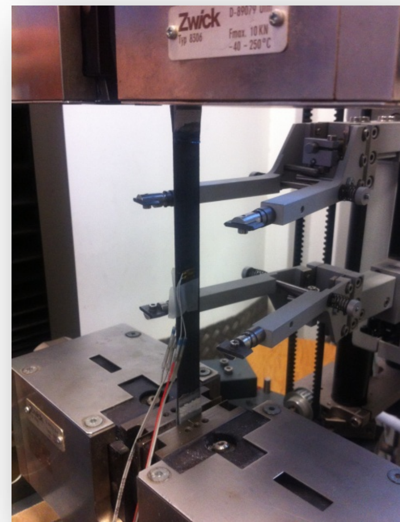

➢ HVI test

Below ballistic limit (projectile rebound)

Above ballistic limit (complete perforation)

High velocity impact (HVI) on composite structures

P.Gaudenzi, L.Lampani

2. ***Development, implementation and validation*** of a ***new analitical model*** to predict resistance to HVI of thin structures (ballistic limit) and the damage size induced by different damage mechanisms.

Below ballistic limit

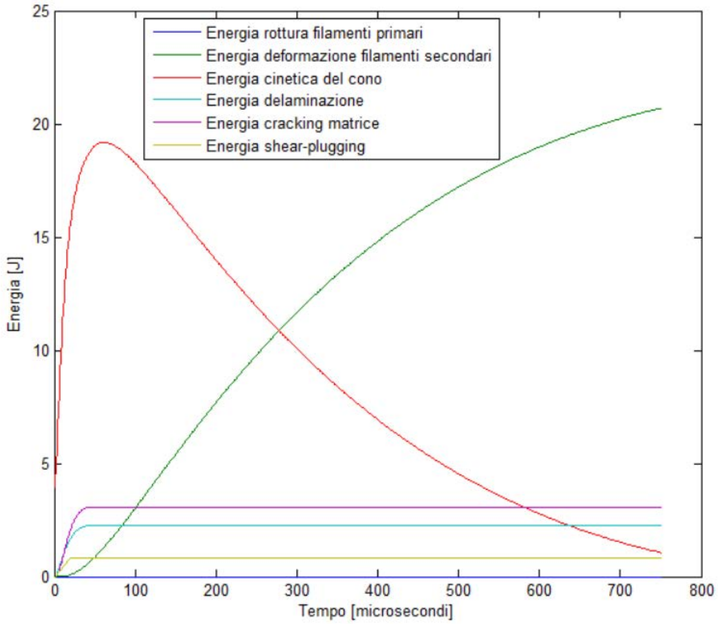

Above ballistic limit

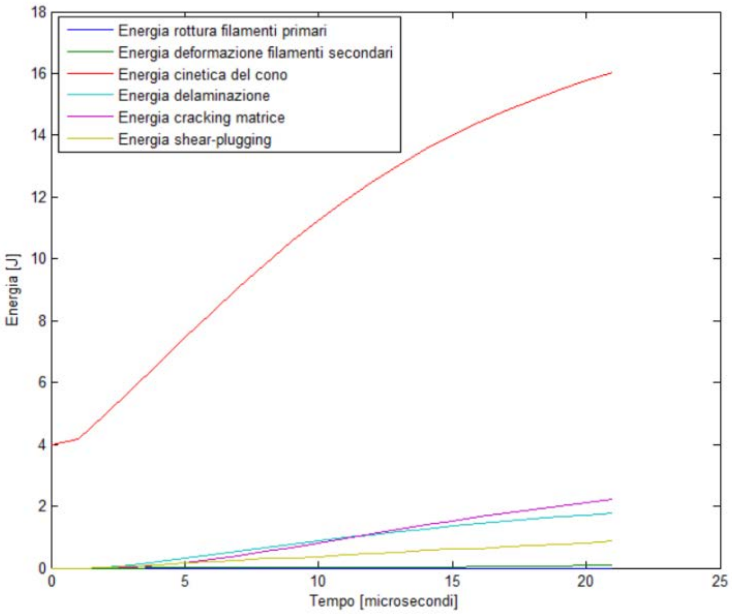

- Good correlation between the experimental and analitical results.

	Numerical result	Experimental result
Ballistic limit [m/s]	181	174

Low velocity impact (LVI) on composite structures

P.Gaudenzi, L.Lampani

Numerical model realization for:

1. Low-velocity impact dynamic simulations [1]
2. Piezoelectric sensor positioning

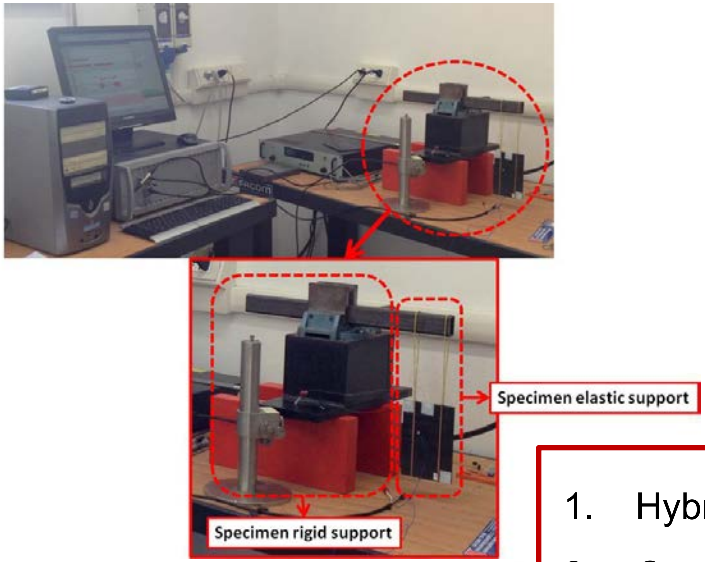

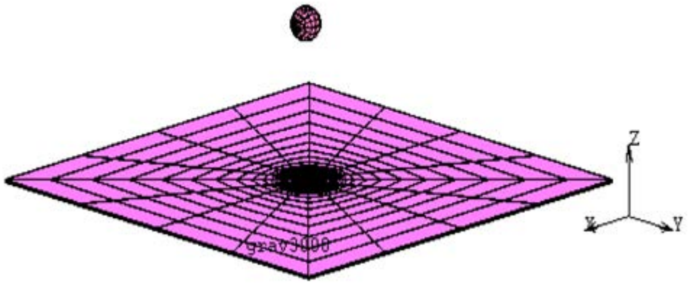

Drop-weight tests for:

1. Hybrid material impact behaviour investigation [2]
2. Comparison between Non Destructive Techniques (NDT) [3]
3. Investigation on modal analysis and wavelet theory as new NDT

[1] *"Numerical simulation of delamination induced by drop-weight impact in composite space structures and correlation with experimental data"* M.Flaccovio, L.Lampani, P.Gaudenzi, 65th Int. Astronautical Congress, Toronto, Canada – 2014.

[2] *"Drop-weight impact behaviour of woven hybrid basalt-carbon/epoxy composites"* - F.Sarasini, J.Tirollò ,L..Ferrante, T.Valente, L.Lampani, P. Gaudenzi , S.Cioffi,S.Iannace,L.Sorrentino, Composites ,Vol.59, 204-220, 2014

[3] *"On the evaluation of impact damage on composite materials by comparing different NDI techniques "* – P. Gaudenzi, M.Bernabei, E.Dati, G. De Angelis , M.Marrone, L.Lampani, Composites , Structures ,Vol.118, 257-266, 2014

LVI numerical simulation and NDT comparison

P. Gaudenzi, L. Lampani

LVI numerical simulation:

1. Static and Dynamic analysis
   Boundary

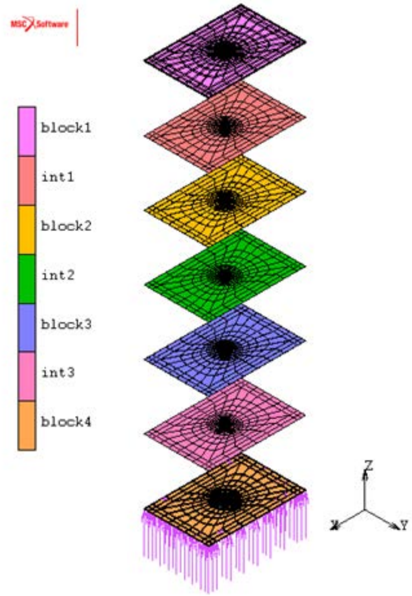

Hybrid Materials behaviour:

1. Drop-weight impact tests
2. Interlaminar shear strength evalauation
3. Residual mechanical properties investigation
4. Damage tollerance evaluation

NDT comaprison:

1. Optical Thermography
2. Ultrasoinic Phased Array
3. Sonic Infrared Thermography

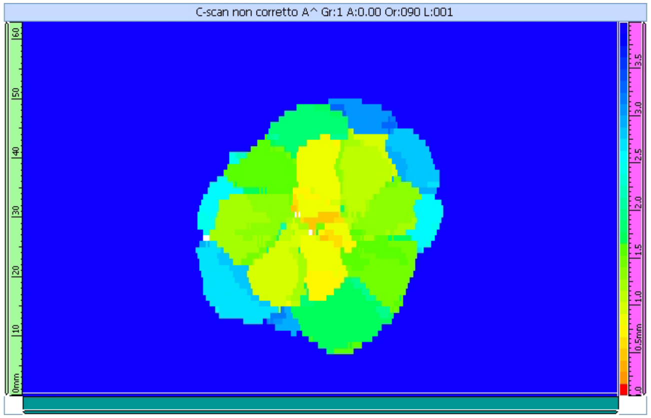

Damage detection on sensorized composite structures subjected to LVI

P. Gaudenzi, L. Lampani

Experimental activities:

•Damage detection via modal analysis and wavelet theory.

Modal Analysis damage indicators:

1. Frequencies shift
2. Mode shape variation
3. Curvature variation

Frequencies shift

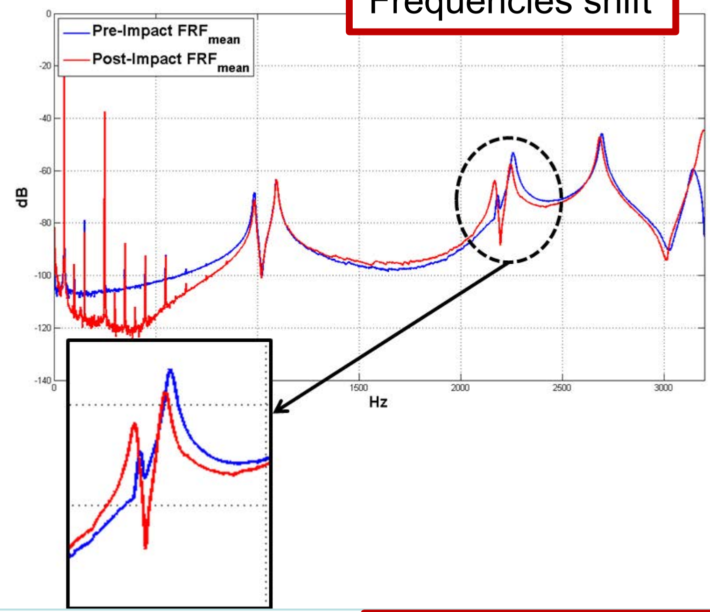

Sensorized Specimen

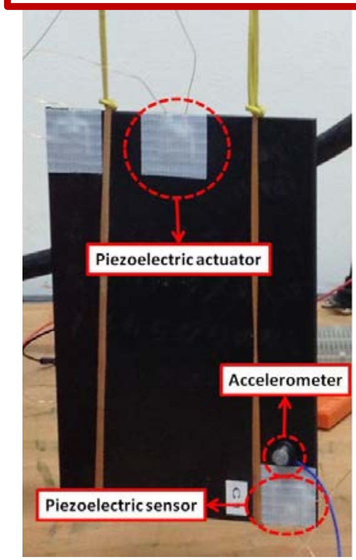

Mode shape comparison after LVI

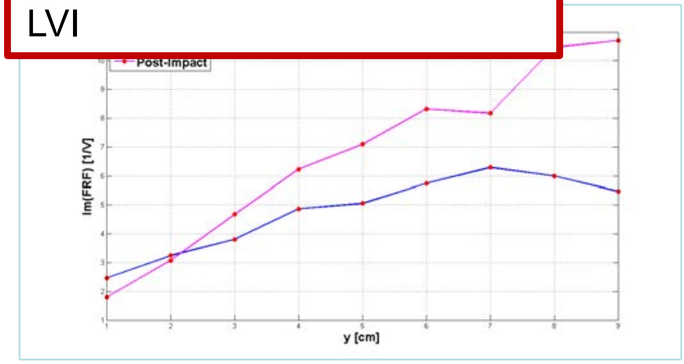

Specimen FEM model

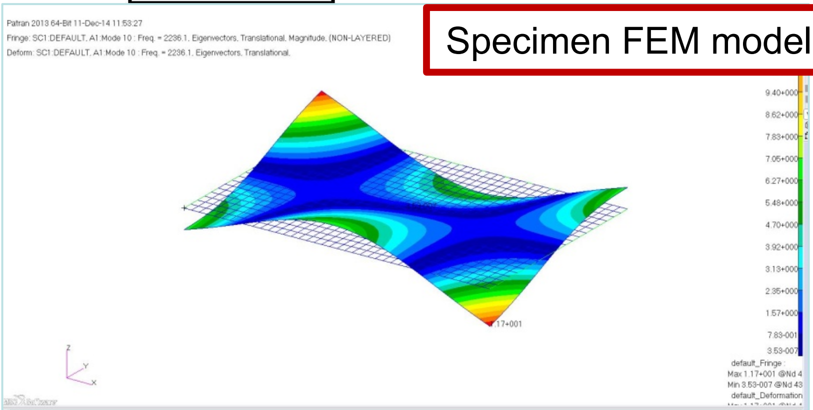

Wavelet Packet transform for Structural Health Monitoring purposes

A Wavelet Packet transform (WPT) based procedure has proved to be effective for the identification and classification of the damaged configurations of test case structures.

- Time domain *vibrating response* of the structure is acquired through a limited amount (1-4) of sensors (i.e. accelerometers).

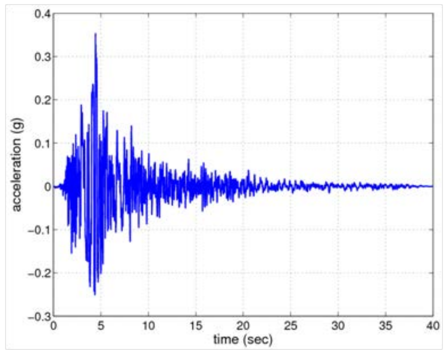

- The acquired time histories have been processed to extract their wavelet packet coefficients $w_{j,k,n}$

$$\psi_{a,\tau}(t) \equiv \frac{1}{\sqrt{|a|}}\,\psi\left(\frac{t-\tau}{a}\right)$$

$$a > 0$$

$$\tau \in \mathbb{R}$$

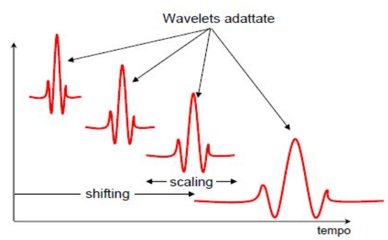

$$\psi^{n}_{j,k}(t) = 2^{j/2}\,\psi^{n}(2^{j}t-k)$$

$$w_{j,k,n} = \int x(t)\,\psi^{n}_{j,k}{}^{*}(t)\,dt$$

- The energy of every wavelet packet $e_{j,n}$, cannot be directly used as effective *damage sensitive features*.

$$e_{j,n} \equiv \sum_{k} w^{2}_{j,k,n}$$

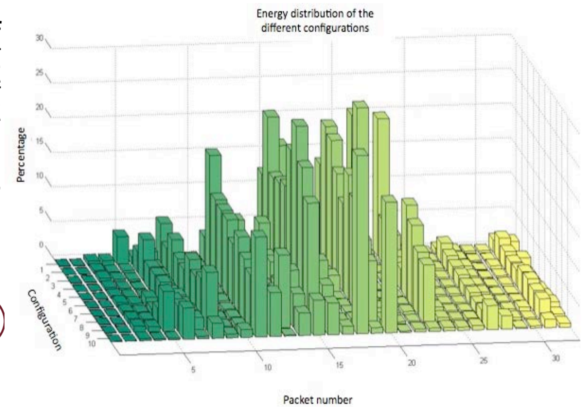

- Linear Discriminant Analysis (LDA): statistical tool employed to project the energy of the wavelet packets in a pattern recognition suitable sub-space

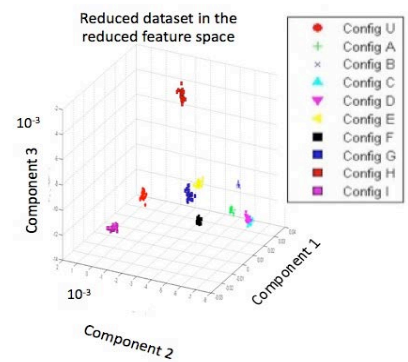

Wavelet Packet transform for Structural Health Monitoring purposes

Applications developed (2/2)

Aluminum truss-type structure:

- 3 accelerometer sensors placed on the last level of the structure and 1 accelerometer placed on the third level;
- 9 mass variation based damaged configurations (percentage variation of mass from 3% to 12%).

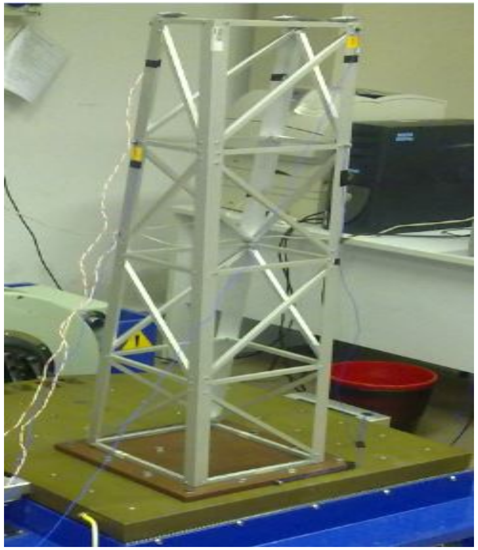

Identification rate of success, third accelerometer (%)

Training Set Samples	5	10	15	20
Configuration				
U	100	100	100	100
A	100	100	100	100
B	100	100	100	100
C	90	100	100	90
D	95	85	95	95
E	95	100	100	100
F	100	100	100	100
G	100	95	100	100
H	100	100	100	100
I	100	100	100	100

Innovative Materials

C. Scarponi

Growing environmental concerns have sparked renewed interest in the development of natural-fibre composites (NFC) and biodegradable materials, which could be the new eco-friendly alternative to fibre-reinforced plastics (Green Composites) with low carbon footprint. **Those are non-toxic, low-cost environmentally sustainable materials that are easily available and help making the workplace healthier**

Kenaf

Hemp

Flax

Innovative Materials

C. Scarponi

The many advantages of these materials include specific mechanical properties, **good thermal, acoustic and electrical insulating properties, low density**, reduced tool wear, excellent deformability, and **safe crash behavior** (no splintering). Consequently, natural fibers (NF) can be used as a **low-cost reinforcement alternative to glass fibers**. Considering that it is possible to use the same processes, tools, labor, equipment, controls and know-how, an easy substitution is possible in short time at reasonable cost.

Fibre	Density [g/cm3]	Elongation [%]	Tensile strenght [MPa]	Young's modulus [GPa]
Cotton	1,5-1,6	7,0-8,0	287-597	5,5-12,6
Jute	1,3	1,5-1,8	393-773	26,5
Flax	1,5	2,7-3,2	345-1035	27-85
Hemp	1,4	1,6	400-1000	25 - 50
Ramie	-	3,6-3,8	400-938	61,4-128
Sisal	1,5	2,0-2,5	511-635	9,4-22,0
Soft Wood	1,5	-	1000	40,0
Glass	2,5	12,5	2000-3000	70,0
Aramid	1,4	3,3-3,7	3000-3150	63,0-67,0

Innovative Materials

C. Scarponi

data about natural fibers production in the world

Examples of non aeronautical applications

Fiber	*Country*	*Production (1000 ton)*	*Percent age of world's produc rion*	*Years*	*World's Producti on (1000 ton)*	*Price ($/Kg) ** *
Jute	India	1533	62.19	2001/ 02- 04/05	2465	0.35 (1.5/0.9-2)
	Banglades h	872.75	35.4			
	Nepal	16.83	0.61			
Flax	UE (Especially France 74% e Belgio 15%)		20*	2006	751 (yr 2004)	0.5–1.5 (2/4)
	Canada		26*	2004		
	USA		13*			
	China		21*			
	India		11*			
Hemp	Cina		39*	2004	83 (yr 2004)	0.6–1.8 (2/4)
	EU (France 55%, UK 11%, Romania 10%, Germany 8%, Czech Republic 7%, e Poland 5%)		9*	2006		

*percentuage of world's area dedicated to the relative cultivation;
**approximate values; strongly dependent by: period, country and allotment's dimension.

Innovative Materials

C. Scarponi

Application of natural fibers in Ultralight Aviation (out of certification procedures): rudder and naca engine
Materials: hemp fabric/epoxy

Rudder

Naca engine

Suggestion: Improve the research on hemp and flax composite materials

Future application are in civil aviation interiors.

Stowage bins

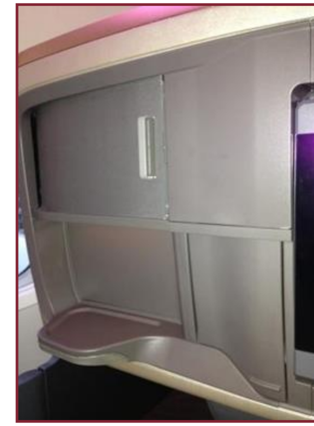

Side panels

Toilette

Utilities

The Concurrent Design Facility (CDF)

P. Gaudenzi

Concurrent Design (CD) is a methodology that allows the parallel design of several subsystems, managing their mutual interactions, which are then assembled to form an engineering system. The use of this methodology is particularly useful in aerospace engineering, where the design is challenged by the presence of very complex engineering systems.
La Sapienza CDF software has been developed in compliance with the European Space Agency's directions.

Examples of Missions Developed with the CDF

- **GEO TLC satellite**
- **LEO SAR satellite**
- **EO Scientific mission constellation**
- **EO mission for the monitoring of catastrophic events**
- **Lunar Observation Mission**
- **Interplanetary mission for the exploration of Titan**
- **LEO constellation for client-missions' data relay**

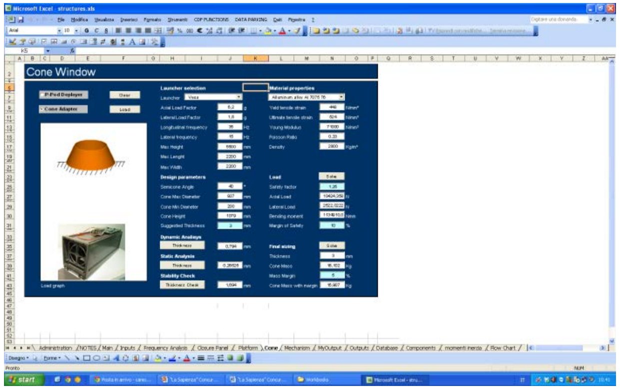

CDF's architecture is based on inter-linked Excel WorkBooks.

- **1 WorkBook for each subsystem:**
  - **AOCS**
  - **Data Handling**
  - **Payload**
  - **Power**
  - **Propulsion**
  - **Structure**
  - **TT&C / Telecommunications**
  - **Thermal**
- **1 Mission WorkBook**
- **1 System Workbook**
- **1 Configuration WorkBook**
- **1 Data Exchange Workbook**

- **The CDF interacts with other professional software**
  - STK
  - AutoCAD Inventor
  - PRICE
  - Structural analysis software (ADINA, …)

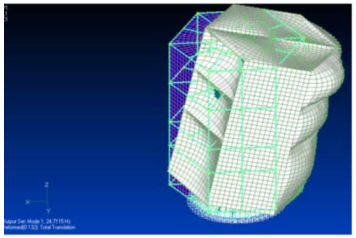

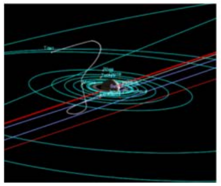

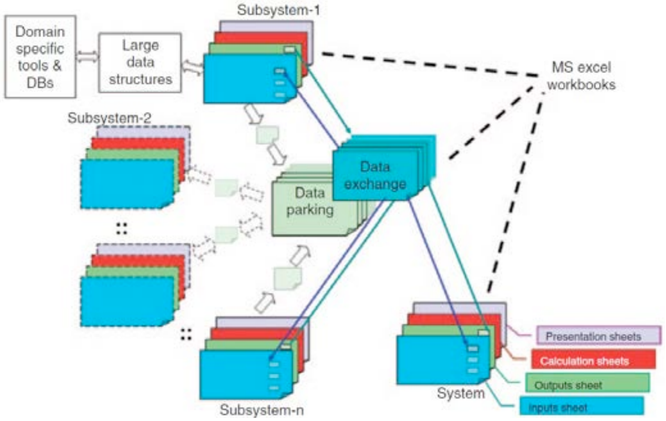

The Concurrent Design Facility (CDF): TALE

P. Gaudenzi

- Tale consists in an interplanetary mission to travel towards Titan and land on one of its lakes
- Its primary mission objectives are:
  - Determine the presence of complex organic molecules in Titan's lakes and seek for biomarkers of extraterrestrial life
  - Determine the chemistry of seas, looking for the abundance of constituents in the liquids and analyze the amino acids' chirality present in Titan's sea.
  - Measure the lake characteristics, streams and tides and map its bottom.
  - Count lightning in Titan's atmosphere to correlate them to the measured chirality.
  - Determine temperature and pressure at surface level.

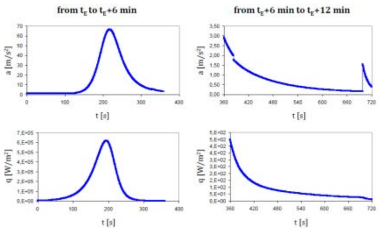

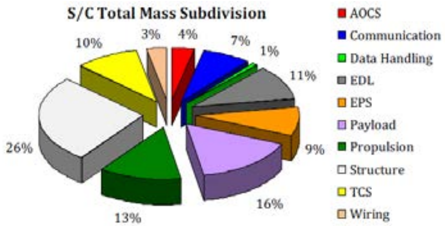

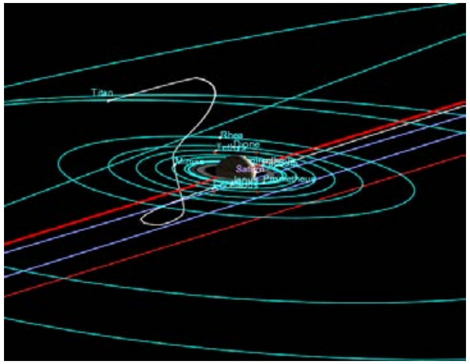

The final spacecraft design is composed by three modules:

- Service Module, used during the interplanetary cruise;
- Entry, Descent & Landing Module, used to protect the Lander Module during the atmospheric phase;
- Lander Module, used to host the bus and the payload and to protect them from the external environment.

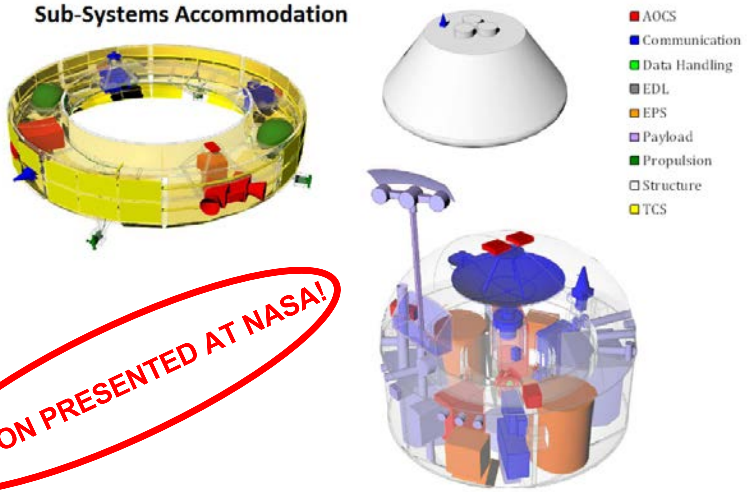

MISSION PRESENTED AT NASA!

The Concurrent Design Facility (CDF): E.O.S.S. : Earth Orbiting Support System

- The study proposed a Low Earth Orbiting constellation as a data relay backbone intended to support client LEO satellites in Data Transfer and TT&C.

- The infrastructure would, in a "System of Systems" logic, allow instant programming and data transfer, finding the appropriate path to the EO spacecraft (via the appropriate EOSS nodes) wherever it is located around the earth.

- The aim of the proposed infrastructure is to overcome some of the limitations and time-latencies currently existing, especially w.r.t. Earth Observation Missions.

- **The study takes advantage of advanced System Architecting techniques developed at M.I.T. (which are based on the Pareto-optimality principle), to identify, some optimal architectural configuration for the EOSS concept.**

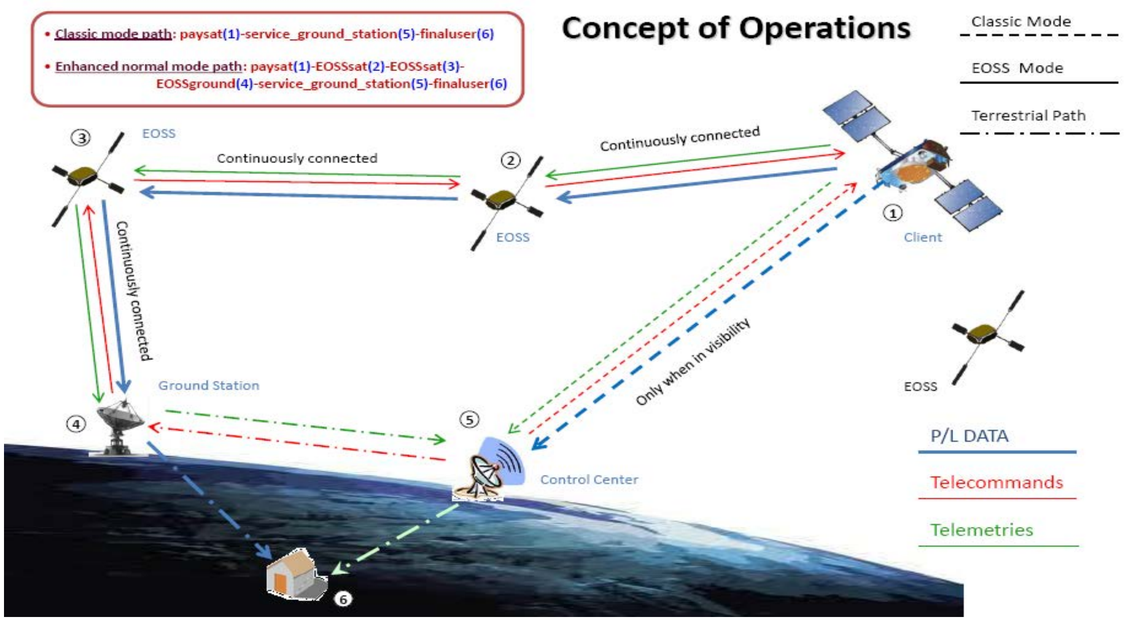

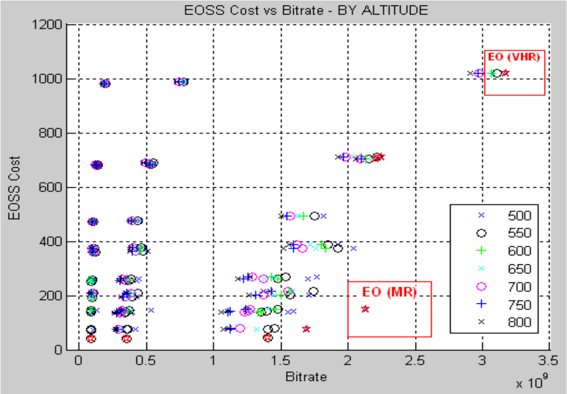

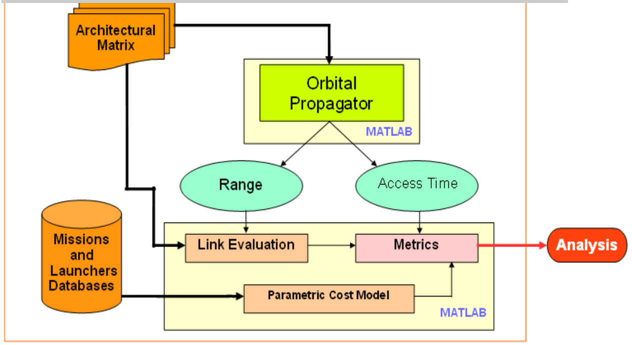

Inverse problems: A two level procedure based on G.A to optimize and aeronautical composite structure

P.Gasbarri

Joint Research: Universitity of the Sinos Valley – UNISINOS (Brazil), University of Rome (Italy), National Institute for Space Research - INPE (Brazil)

L.D. Chiwiacowsky, P. Gasbarri, H.F. Campos Velho, and A.T. Gómez

A wing composite structure is composed of a large number of panels, which have to be designed simultaneously to obtain an optimum structural response. The optimal design of a composite wing-box is addressed by using a two-level scheme, where two different Genetic Algorithms are used to solve each level problem.

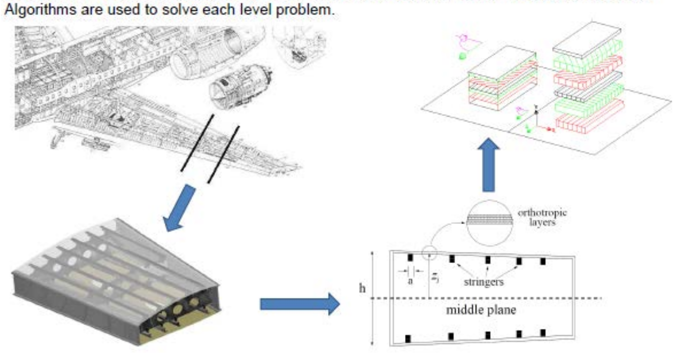

At the upper level the anisotropy parameters are defined by using a real coded genetic algorithm in order to maximize the value of flutter velocity. At the lower level, depending on the degree of anisotropy imposed by the upper level, the composite layers orientation are defined by using a genetic algorithm based on integer encoding.

The Two-Level Optimization Procedure:

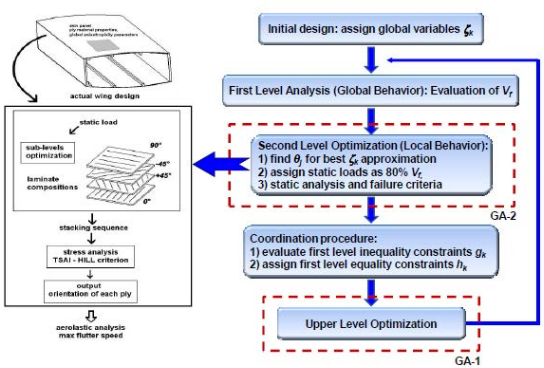

Problem Definition:

The basic formula for studying the aeroelastic phenomena (both static and dynamic) on elastic wings is given by:

$$\mathbf{M}\ddot{\mathbf{X}} + \mathbf{K}\mathbf{X} = q_\infty\, \mathbf{R}\{\alpha_g + \mathbf{Q}\mathbf{X}\} = \mathbf{F}_{aer}$$

The case of symmetric orthotropic laminate is considered, with the orthotropic plate bending stiffness matrix defined as:

$$\mathbf{D} = \mathbf{D}^{00} + \mathbf{H}^{01}\zeta_3 + \mathbf{H}^{02}\zeta_1 + \mathbf{H}^{10}\zeta_4 + \mathbf{H}^{12}\zeta_2$$

where the terms ζ_k are the global design variables, functions of the orientation of the layers of laminate θ_j (j = 1, ..., N_{La}), which are the local design variables to be determined in order to maximize the aerodynamic pressure q_∞ undergoing certain composite failure constraint conditions. The relation between the design variables are defined as:

$$\zeta_1 = \sum_{j=1}^{N_{La}} \frac{z_j^3 - z_{j-1}^3}{3}\cos 4\theta_j \qquad \zeta_3 = \sum_{j=1}^{N_{La}} \frac{z_j^3 - z_{j-1}^3}{3}\cos 2\theta_j$$

$$\zeta_2 = \sum_{j=1}^{N_{La}} \frac{z_j^3 - z_{j-1}^3}{3}\sin 4\theta_j \qquad \zeta_4 = \sum_{j=1}^{N_{La}} \frac{z_j^3 - z_{j-1}^3}{3}\sin 2\theta_j$$

For numerical simulations, the number of layers was assumed N_{La}=6, taken on N_L=5 different locations of the wing span. Therefore, there are 5×6 local variables and 5×4 global variables for a total of 50 design variables to be identified.

First Level Optimization (GA-1)

The problem of maximizing the flutter velocity is transformed into a minimization problem and it is solved by a GA assuming the fitness function defined as follows:

$$\phi_I = w_v \frac{1}{V_f} + \sum_{k=1}^{N_L} w_g \max(0, g_k) + \sum_{k=1}^{N_L} w_h \max(0, h_k)$$

In this expression the equality and inequality constraints were added as penalty functions, where the constants w_v, w_g and w_h are used to balance the terms in the expression. At the first level optimization, a real coded GA is used with the following solution encoding:

$$[\zeta_1^1/\ \zeta_2^1/\ \zeta_3^1/\ \zeta_4^1/\ \zeta_1^2/\ \zeta_2^2/\ \zeta_3^2/\ \zeta_4^2/\ \ldots/\zeta_1^{N_L}/\ \zeta_2^{N_L}/\ \zeta_3^{N_L}/\ \zeta_4^{N_L}]$$

The following genetic operators were used: Tournament Selection, Arithmetic Crossover and Non-uniform Mutation.

Second Level Optimization (GA-2)

For each wingspan location, the orientation angles are sought to provide the stiffness required by the upper level optimization and the strength to withstand loads calculated by the upper level analysis. The fitness function for the second level subproblems is given by:

$$\phi_{II} = \frac{(\zeta_1 - \bar{\zeta}_1)^2 + (\zeta_2 - \bar{\zeta}_2)^2 + (\zeta_3 - \bar{\zeta}_3)^2 + (\zeta_4 - \bar{\zeta}_4)^2}{\bar{\zeta}_1^2 + \bar{\zeta}_2^2 + \bar{\zeta}_3^2 + \bar{\zeta}_4^2}$$

Where barred quantities denote upper level design variables. At the second level optimization, an integer coded GA is used with the following solution encoding:

$$[\theta_1/\ \theta_2/\ \theta_3/\ \theta_4/\ \theta_5/\ \theta_6]$$

The following genetic operators were used: Tournament Selection, Two-point Crossover, Uniform Mutation and Epidemical.

Numerical Results:

The efficiency and robustness of the two-level optimization procedure was evaluated by solving different design problems of a composite laminate of a wing-box according to different choices of the angle variation $\Delta\theta_j$ and transverse stiffness E_{22}.

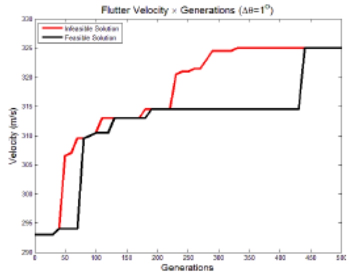

Fig 1: Flutter velocity × generation, $\Delta\theta$=1° and E_{22}=65 Gpa.

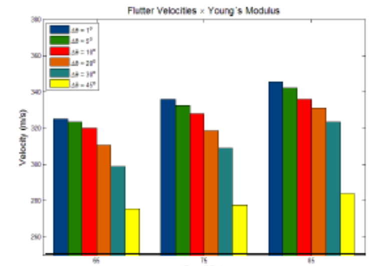

Fig 2: Maximum flutter velocity × Young's Modulus for different $\Delta\theta$ ply orientation.

Multibody Dynamics for space applications
Modeling and control of large flexible space structure
P.Gasbarri

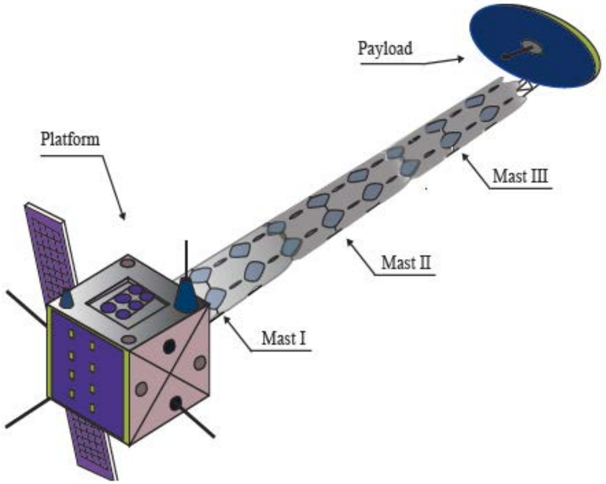

Extra Long Mast Observatory (ELMO) 2018

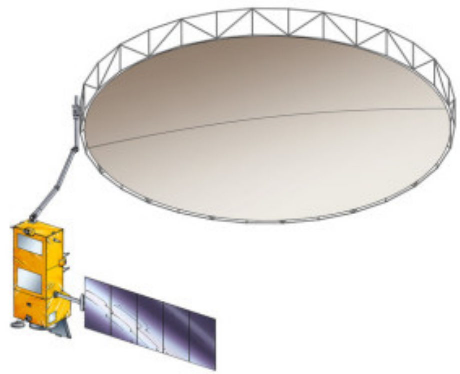

BIOMASS

Multidisciplinary formulation:

Flight Mechanics

Spacecraft Flexibility

Gravitation

Control (orbital, attitude, vibrations)

Multiple scales dynamics → Time

Space

Kinematics…

$$\boldsymbol{r} \equiv \left(\boldsymbol{\xi} + \sum_{k=1}^{N} A_k(t)\boldsymbol{\phi}_k(\boldsymbol{\xi})\right)$$

Center of mass

Modal decomposition

$$\mathbf{X}(P) = \mathbf{X}_0 + \mathbf{T}\left(\boldsymbol{\xi} + \sum_{k=1}^{N} A_k(t)\boldsymbol{\phi}_k(\boldsymbol{\xi})\right)$$

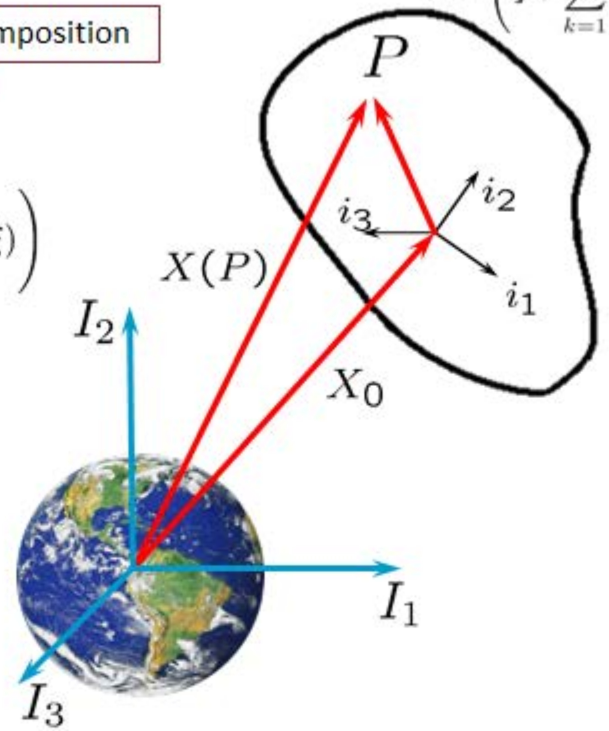

Multibody Dynamics for space applications
Modeling and control of large flexible space structure
P.Gasbarri

Equation of motion…

$$
\begin{cases}
m\ddot{\mathbf{X}}_0 + [\boldsymbol{\omega} \wedge (\boldsymbol{\omega} \wedge \tilde{\mathbf{p}})] + (\dot{\boldsymbol{\omega}} \wedge \tilde{\mathbf{p}}) + \left(2\boldsymbol{\omega} \wedge \sum_{k=1}^{N} \boldsymbol{\Lambda}_k \dot{A}_k\right) + \\
\quad + \sum_{k=1}^{N} \boldsymbol{\Lambda}_k \ddot{A}_k = \mathcal{F}_G \\
\tilde{\mathbf{p}} \wedge \ddot{\mathbf{X}}_0 + \tilde{\mathbf{J}}\dot{\boldsymbol{\omega}} + \sum_{k=1}^{N} \left(\tilde{\mathbf{J}}_1^k \dot{A}_k\right) \boldsymbol{\omega} + \sum_{k=1}^{N} \sum_{t=1}^{N} \boldsymbol{\Xi}^{kt} \dot{A}_t \dot{A}_k + \\
\quad + \sum_{k=1}^{N} \tilde{\boldsymbol{\Gamma}}_k \ddot{A}_k + \boldsymbol{\omega} \wedge \tilde{\mathbf{J}}\boldsymbol{\omega} + \boldsymbol{\omega} \wedge \sum_{k=1}^{N} \tilde{\boldsymbol{\Gamma}}_k \dot{A}_k = \mathcal{C}_G \\
\boldsymbol{\Lambda}_k{}^T \ddot{\mathbf{X}}_0 + \tilde{\boldsymbol{\Gamma}}_k^T \dot{\boldsymbol{\omega}} + \ddot{A}_k + \omega_k^2 A_k + 2\zeta_k \omega_k \dot{A}_k - \frac{1}{2}\boldsymbol{\omega}^T \tilde{\mathbf{J}}^k \boldsymbol{\omega} + \\
\quad + 2\boldsymbol{\omega}^T \sum_{t=1}^{N} \boldsymbol{\Xi}^{kt} \dot{A}_t = \bar{\mathcal{F}}_{G,k} \qquad k = 1, ..., N
\end{cases}
$$

$$\mathcal{F}_G = -m\frac{\mu\hat{k}}{|\mathbf{X}_0|}$$

2

$$\mathcal{C}_G = -\frac{\mu}{|\mathbf{X}_0|^2}\left(\tilde{\mathbf{p}} \wedge \hat{k}\right) + \frac{3\mu}{|\mathbf{X}_0|^3}\left(\hat{k} \wedge \tilde{\mathbf{J}}\hat{k}\right)$$

$$\bar{\mathcal{F}}_{G,k} = -\frac{3\mu}{2|\mathbf{X}_0|^3}\hat{k}^T \tilde{\mathbf{J}}_1^k \hat{k} + \frac{1}{2}\frac{\mu\, tr(\tilde{\mathbf{J}}_1^k)}{|\mathbf{X}_0|^3} - \frac{\mu}{|\mathbf{X}_0|^2}\hat{k}^T \boldsymbol{\Lambda}_k$$

Multibody Dynamics for space applications
Modeling and control of large flexible space structure
P.Gasbarri

Inertial coupling terms…

CONSTANT + **TIME VARYING**

Generalized Mass Matrix

Mass

$$m = \int_{\mathcal{B}} \rho d\mathcal{B}$$

Static Moments

$$\tilde{\mathbf{p}} = \mathbf{p} + \sum_{t=1}^{N} \mathbf{\Lambda}_k A_k = = \int_{\mathcal{B}} \xi \rho d\mathcal{B} + \int_{\mathcal{B}} \boldsymbol{\phi}^k \; \rho d\mathcal{B}$$

Modal Participation Factors in Translation

$$\mathbf{\Lambda}_k = \int_{\mathcal{B}} \boldsymbol{\phi}^k \; \rho d\mathcal{B}$$

Moments of Inertia

$$\tilde{\mathbf{J}} = \mathbf{J}_0 + \sum_{k=1}^{N} \mathbf{J}_1^k A_k + \sum_{k=1}^{N} \sum_{t=1}^{N} \mathbf{J}_2^{kt} A_t A_k =$$

$$= \int_{\mathcal{B}} (\mathbf{x}^{\mathbf{T}}\mathbf{x} - \mathbf{x}\mathbf{x}^{\mathbf{T}}) \; \rho \mathrm{d}\mathcal{B} +$$

$$+ \sum_{k=1}^{N} \int_{\mathcal{B}} (2\delta_{lm}\xi_j\phi_j^k - \xi_l\phi_m^k - \xi_m\phi_l^k) \; \rho d\mathcal{B} A_k +$$

$$+ \sum_{k=1}^{N} \sum_{t=1}^{N} \int_{\mathcal{B}} (\delta_{lm}\phi_j^k\phi_j^t - \phi_l^k\phi_m^t) \; \rho d\mathcal{B} A_t A_k$$

Modal Participation Factors in Rotation

$$\tilde{\mathbf{\Gamma}}_k = \mathbf{\Gamma}_{0,k} + \sum_{t=1}^{N} \mathbf{\Xi}^{kt} A_k = = \int_{\mathcal{B}} \boldsymbol{\xi} \wedge \boldsymbol{\phi}^k \; \rho d\mathcal{B} + \int_{\mathcal{B}} \boldsymbol{\phi}^k \wedge \boldsymbol{\phi}^t \; \rho d\mathcal{B}$$

Matrix form of the equation of motion :

$$\mathbf{M}\ddot{\mathbf{S}} + \mathbf{C}\dot{\mathbf{S}} + \mathbf{K}\mathbf{S} + \mathbf{N_L} = \mathbf{F}$$

$$\mathbf{S}^T \equiv [\mathbf{X}_0, \mathbf{Q}, \mathbf{A}]$$

$$\left\{\begin{array}{c} \dot{\mathbf{x}}_0 \\ \dot{\mathbf{Q}} \\ \dot{A}^k \\ \hline \ddot{\mathbf{x}}_0 \\ \dot{\boldsymbol{\omega}} \\ \ddot{A}^k \end{array}\right\} = \left[\begin{array}{ccc|ccc} \mathbf{0} & \mathbf{0} & \mathbf{0} & \mathbf{I} & \mathbf{0} & \mathbf{0} \\ \mathbf{0} & \mathbf{0} & \mathbf{0} & \mathbf{0} & \frac{1}{2}\mathbf{Q}^{\mathbf{q}} & \mathbf{0} \\ \mathbf{0} & \mathbf{0} & \mathbf{0} & \mathbf{0} & \mathbf{0} & \mathbf{I} \\ \hline & -\mathbf{M}^{-1}\mathbf{K} & & & -\mathbf{M}^{-1}\,\mathbf{C} & \end{array}\right] \left\{\begin{array}{c} \mathbf{x}_0 \\ \mathbf{Q} \\ A^k \\ \hline \dot{\mathbf{x}}_0 \\ \boldsymbol{\omega} \\ \dot{A}^k \end{array}\right\} + \left\{\begin{array}{c} \mathbf{0} \\ \mathbf{0} \\ \mathbf{0} \\ \hline -\mathbf{M}^{-1}\mathbf{N}_L \end{array}\right\} + \left\{\begin{array}{c} \mathbf{0} \\ \mathbf{0} \\ \mathbf{0} \\ \hline \mathbf{M}^{-1}\mathbf{F} \end{array}\right\}$$

… with the non-linear terms given by:

$$\mathbf{N}_L = \left\{\begin{array}{c} \mathbf{0} \\ \sum_{k=1}^{N} \tilde{\mathbf{J}}_1^k \dot{A}^k \boldsymbol{\omega} + \sum_{k=1}^{N} \sum_{t=1}^{N} \boldsymbol{\Xi}^{kt} \dot{\boldsymbol{A}}^t \dot{\boldsymbol{A}}^k + \boldsymbol{\omega} \wedge \tilde{\mathbf{J}}\boldsymbol{\omega} + \boldsymbol{\omega} \wedge \sum_{k=1}^{N} \boldsymbol{\Gamma}_1^k \dot{A}^k \\ -\frac{1}{2}\boldsymbol{\omega}^T \tilde{\mathbf{J}}_k^1 \boldsymbol{\omega} + 2\boldsymbol{\omega}^T \sum_{t=1}^{N} \boldsymbol{\Xi}^{kt} \dot{A}^t \end{array}\right\}$$

Multibody Dynamics for space applications
Modeling and control of large flexible space structure
P.Gasbarri

Modeling and control large flexible space structure

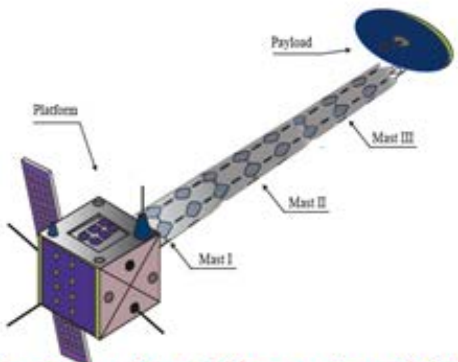

Extra Long Mast Observatory (ELMO) 2018

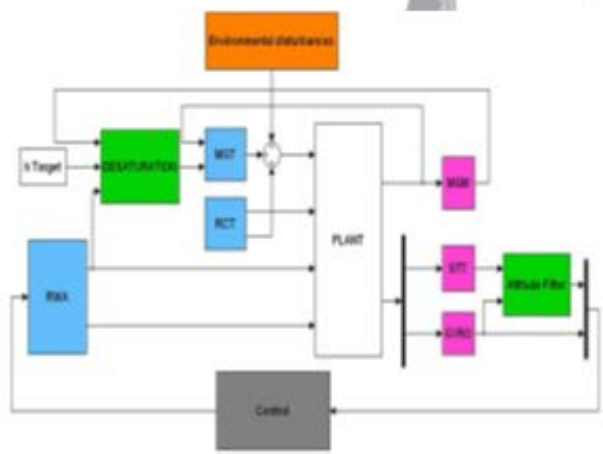

Schematic of the E2E simulator.

Control-oriented modelization of a satellite with large flexible appendages and use of worst-case analysis to verify robustness to model uncertainties of attitude control, Acta Astronautica, Volume 81, Issue 1, December 2012, Pages 214-226, in collaboration with TASI

Multibody Dynamics for space applications
Modeling and control of large flexible space structure
P.Gasbarri

Example: large flexible satellite

Effects of uncertainties and flexible dynamic contributions on the control of a spacecraft full-coupled model, Acta Astronautica, Volume 94, Issue 1, January–February 2014, Pages 515-526

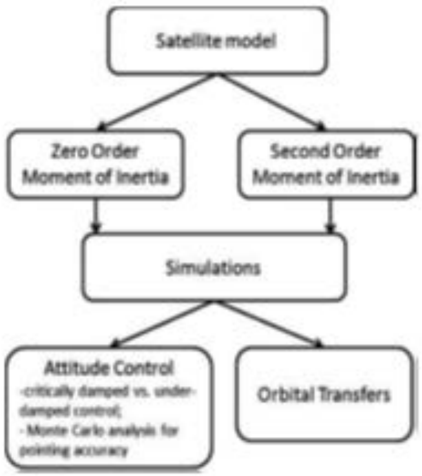

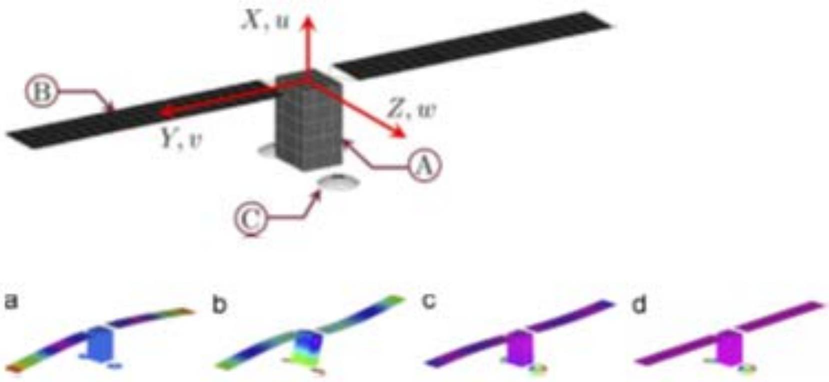

Modal shapes

Multibody Dynamics for space applications
Modeling and control of large flexible space structure
P.Gasbarri

Example: large flexible satellite and stability

Effects of uncertainties and flexible dynamic contributions on the control of a spacecraft full-coupled model, Acta Astronautica, Volume 94, Issue 1, January–February 2014, Pages 515-526

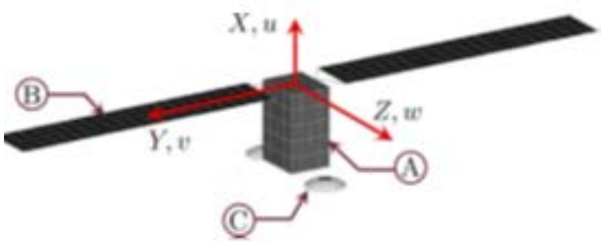

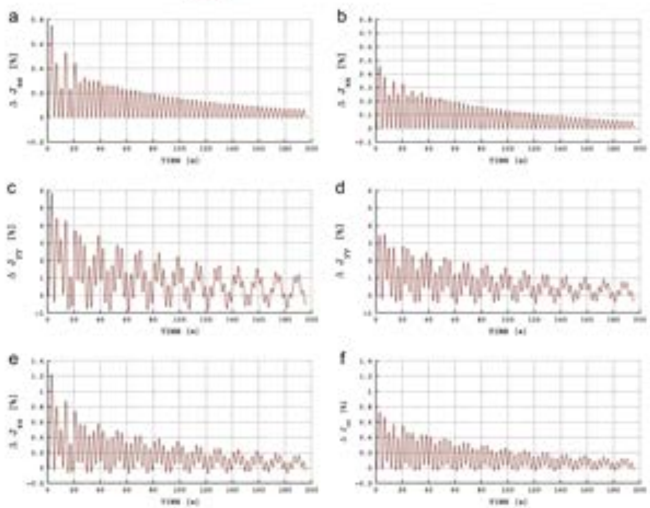

Fig. 7. Percentage variation of the moment of inertia due to the second order coupling. (a) ΔJ_{xx} at $\zeta_i = 0.5$. (b) ΔJ_{xx} at $\zeta_i = 1$. (c) ΔJ_{yy} at $\zeta_i = 0.5$. (d) ΔJ_{yy} at $\zeta_i = 1$. (e) ΔJ_{zz} at $\zeta_i = 0.5$ and (f) ΔJ_{zz} at $\zeta_i = 1$.

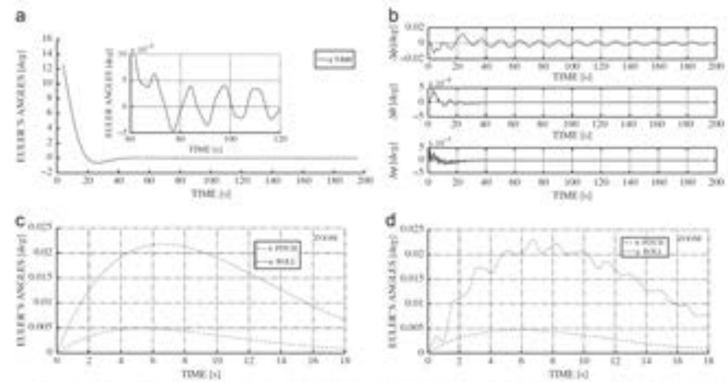

Fig. 4. Euler's angles: comparison between zero order and second order coupling, $\zeta_i = 0.5$. (a) Yaw angle: Second order coupling. (b) Euler's angles variation. (c) Pitch and Roll angles: Zero order coupling and (d) Pitch and Roll angles: Second order coupling.

From stability of flexible spacecrafts to the stability of large flexible aircrafts

Studio degli Effetti della Flessibilità sul Comportamento Dinamico di un Velivolo Wide-Body

(Andrea Polomini Master Thesis 2011)

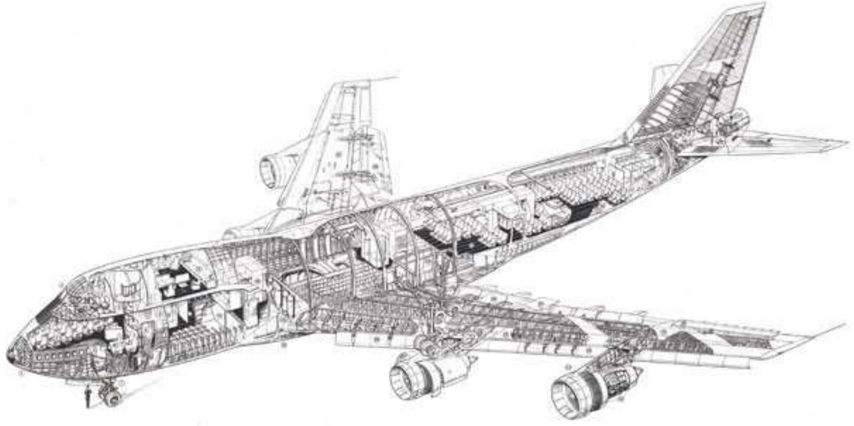

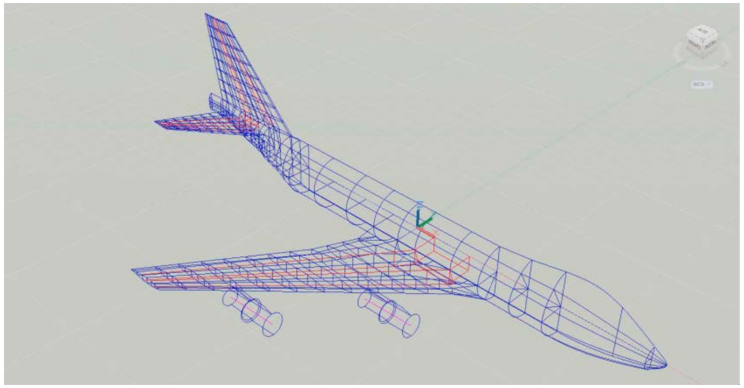

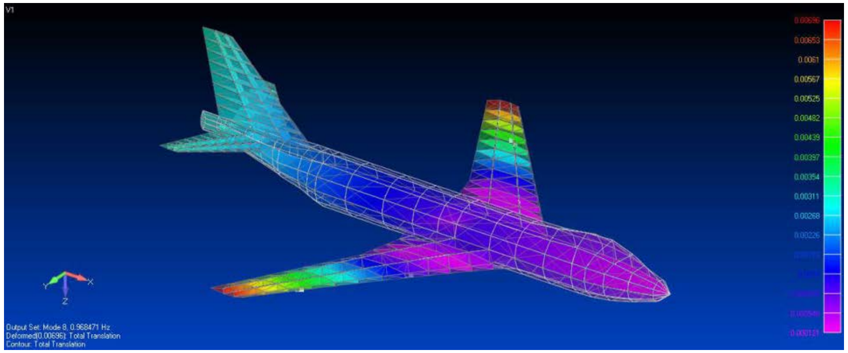

From stability of flexible spacecrafts to the stability of large flexible aircrafts

Modal shapes of a wide – body aircraft

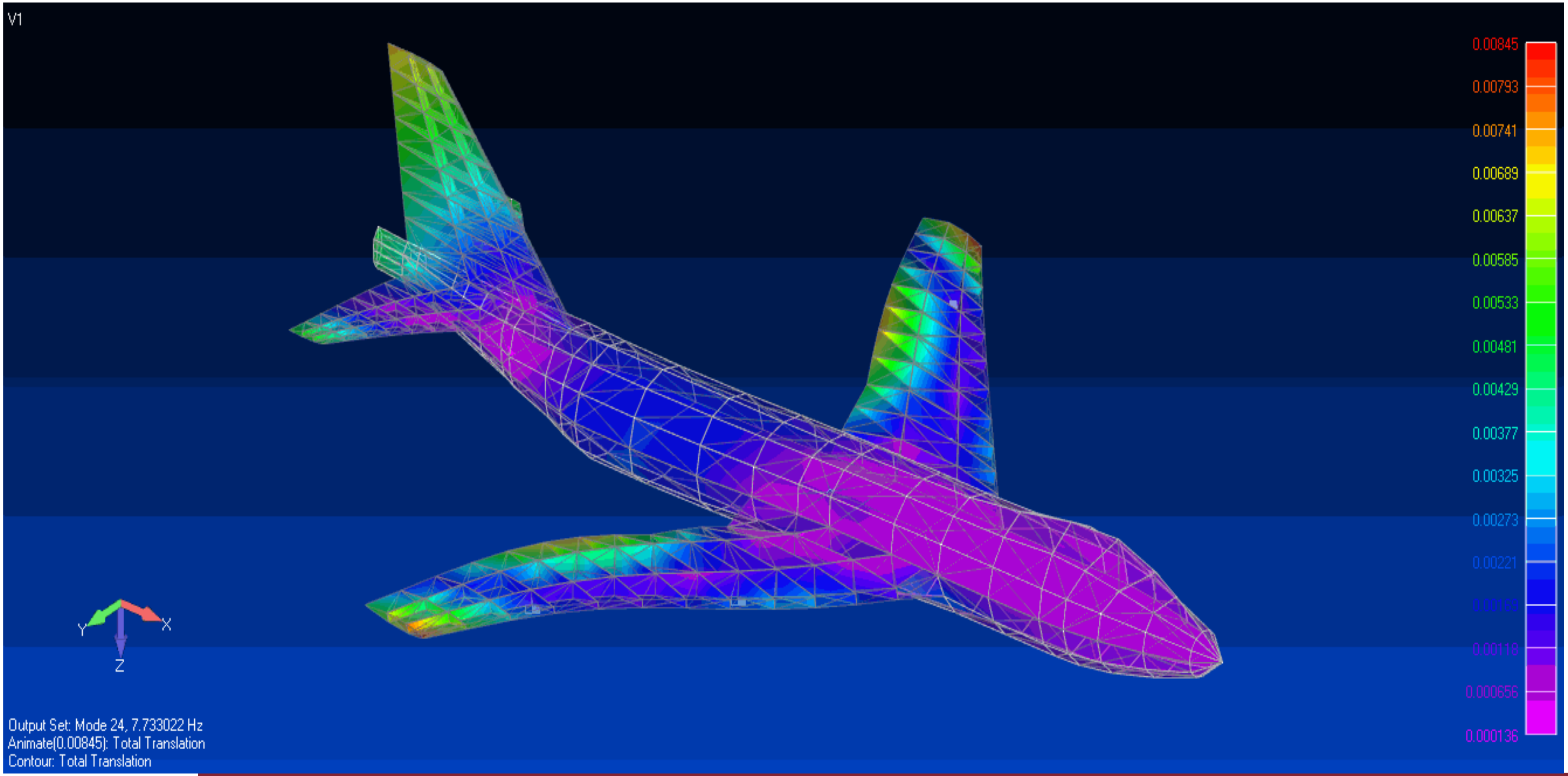

From stability of flexible spacecrafts to the stability of large flexible aircrafts

Study of the full coupled aero-servo-elastic maneuvers

1) **Stability analysis of the full coupled model**
2) **Gust response**
3) **Controlled maneuvers**

Instability rigid+elastic

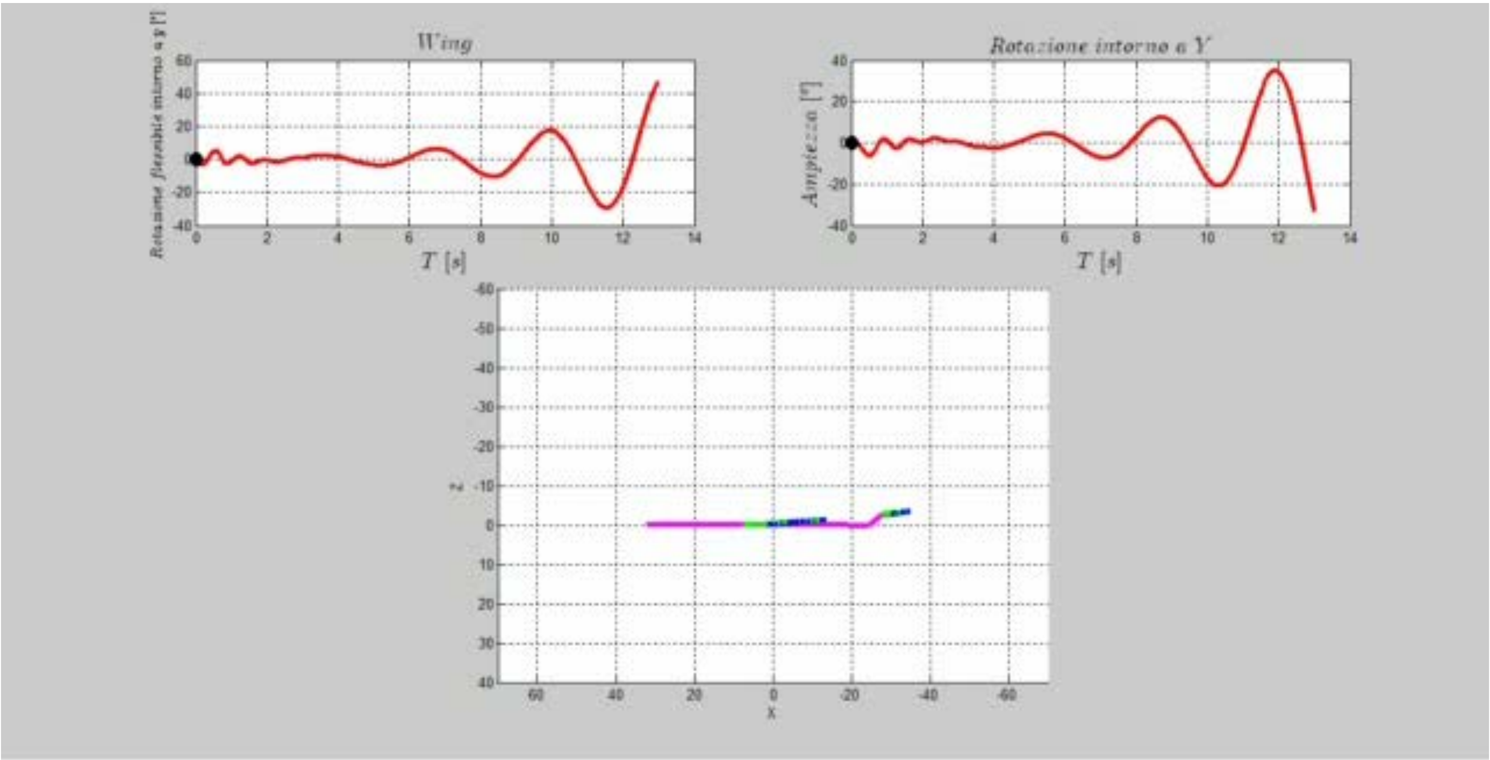

From stability of flexible spacecrafts to the stability of large flexible aircrafts

Study of the full coupled aero-servo-elastic maneuvers

1) **Stability analysis of the full coupled model**
2) **Gust response + control**
3) **Controlled maneuvers**

Instability elastic

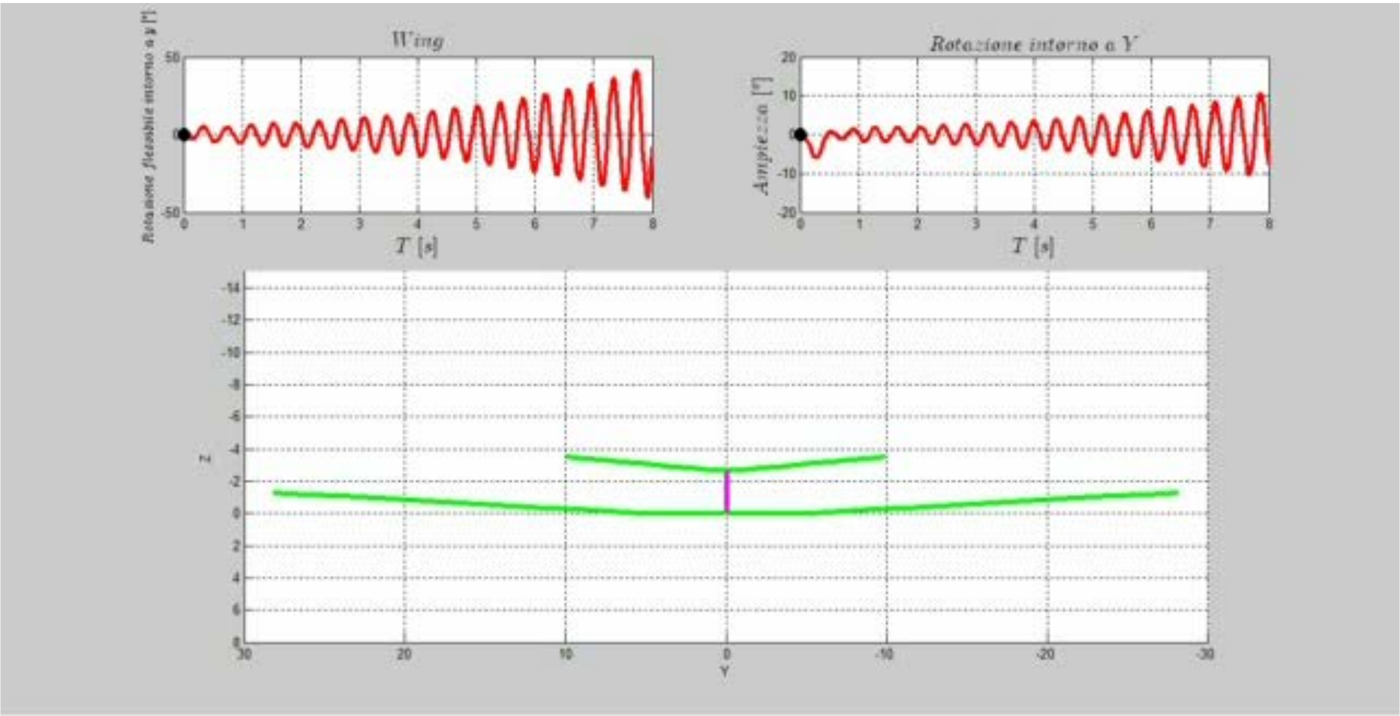

Multibody Dynamics for space applications
Modeling and control of large flexible space structure

P.Gasbarri

Flight Dynamics Numerical Computation of a Sounding Rocket Including Elastic Deformation Model (AIAA Atmospheric Flight Mechanics Conference- 22-26 June 2015, Dallas, TX. Elcio Jeronimo de Oliveira, Paolo Gasbarri, 2014)

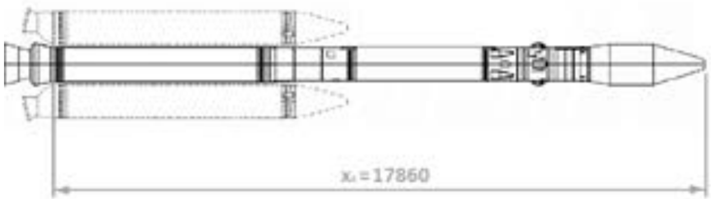

Figure 1.2 - Brazilian VLS with central body highlighted.

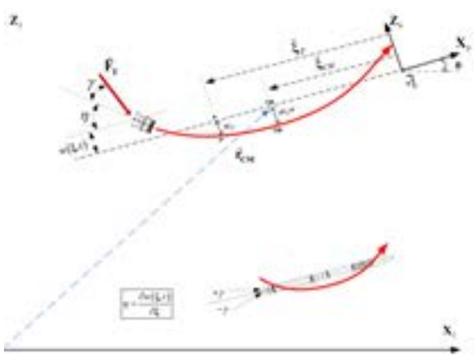

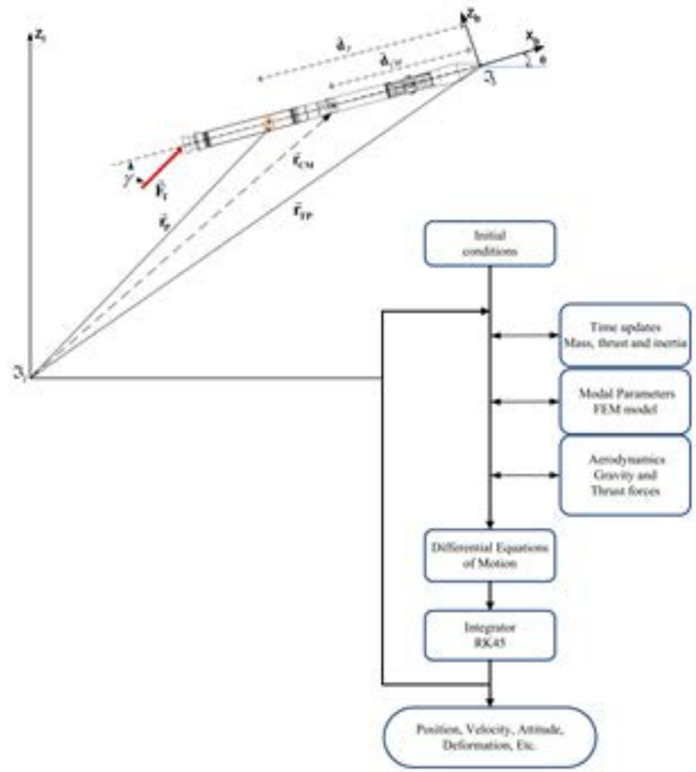

Existing Multibody Approaches

- ***Lagrangian Formulations***
- ***Newtonian Formulations***
- ***Hybrid Formulations (partially Lagrangian and Eulerian)***

Hybrid Multibody Formulation

The Idea:

- Starting from the **Newtonian** formulation (which allows a simple definition of bodies' equations of motion and of the joint constraints), it is possible reduce the system equation of motion to a system by a **minimum set of variables and equations**, such as obtained starting from an **Lagrangian** approach.

Advantage:

- **modularity** of the Newtonian approach for obtaining a system of differential equation without the intrinsic round of errors during the simulations (fully ODE system)
- The proposed procedure allows the shifting from the one to the other approach in order to better analyze the behavior of a multibody system

Procedure:

- This is possible by the definition of the **Jacobian matrix** which allows to calculate the **velocities in the Cartesian** $\dot{\mathbf{X}}$ space as a function of the multibody **joint velocities** $\dot{\mathbf{Q}}$:

$$\dot{\mathrm{X}} = \mathbf{J}\,\dot{\mathrm{Q}}$$

Drawbaks:

The evaluation of the Jacobian matrix needs some algebra to be performed in advance

Space robotics:

P.Gasbarri

DYNAMIC/CONTROL INTERACTIONS BETWEEN FLEXIBLE ORBITING SPACE-ROBOT DURING GRASPING, DOCKING AND POST-DOCKING

Operation design

1. optimal links deployment → Open loop optimization algorithms
2. optimal transfer of the target to the platform
3. grasping of the target → Closed loop robust controllers (LQR, FLT, PD)
4. hold position

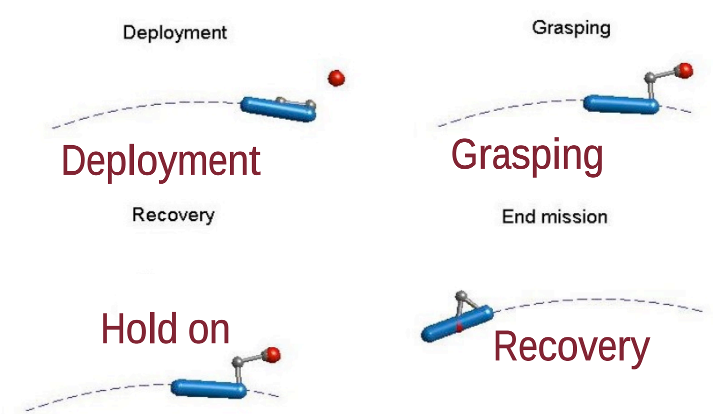

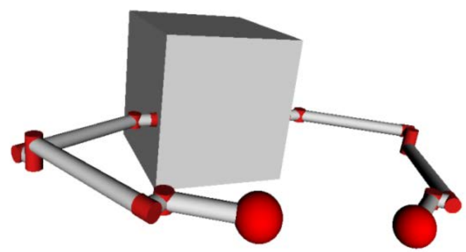

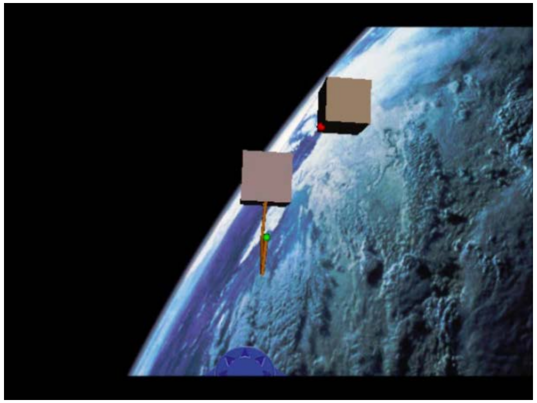

Possible control strategies for deploying the links :

a) Jacobian Transpose Control

b) Reaction Null Jacobian Transpose Control

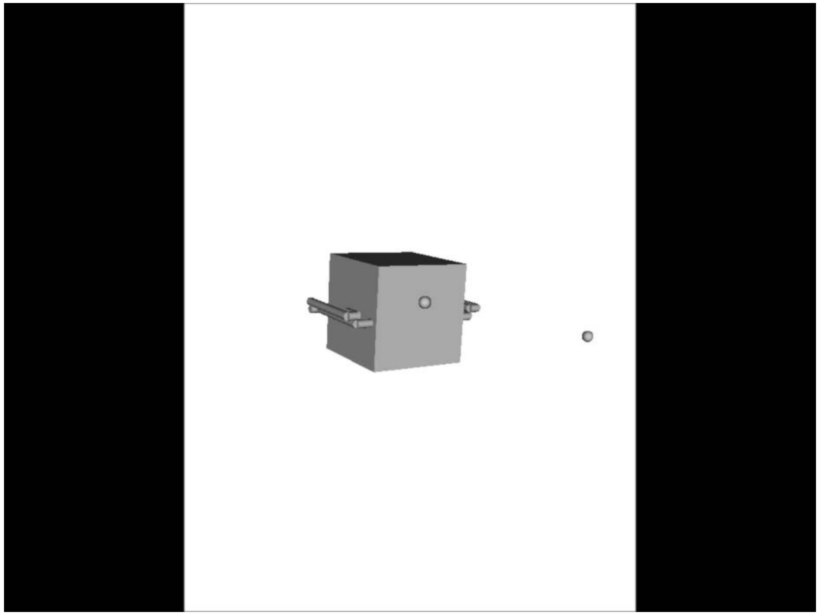

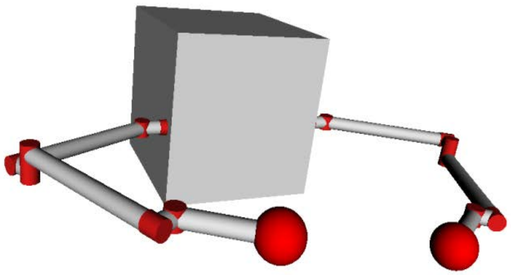

Space robotics:

P.Gasbarri

DYNAMIC/CONTROL INTERACTIONS BETWEEN FLEXIBLE ORBITING SPACE-ROBOT DURING GRASPING, DOCKING AND POST-DOCKING

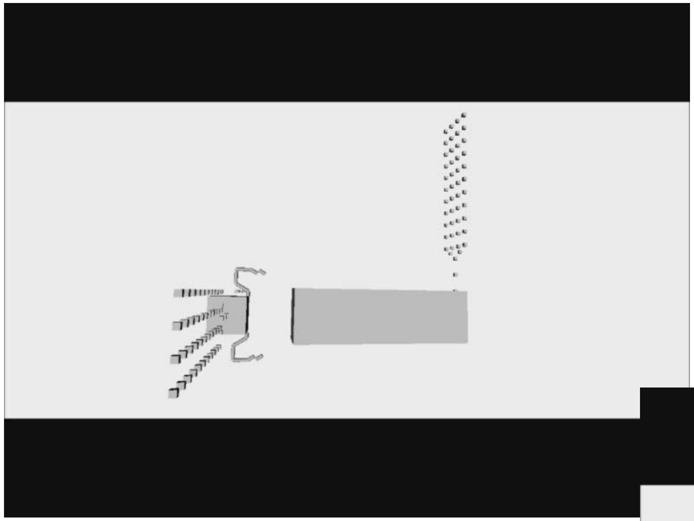

JTC

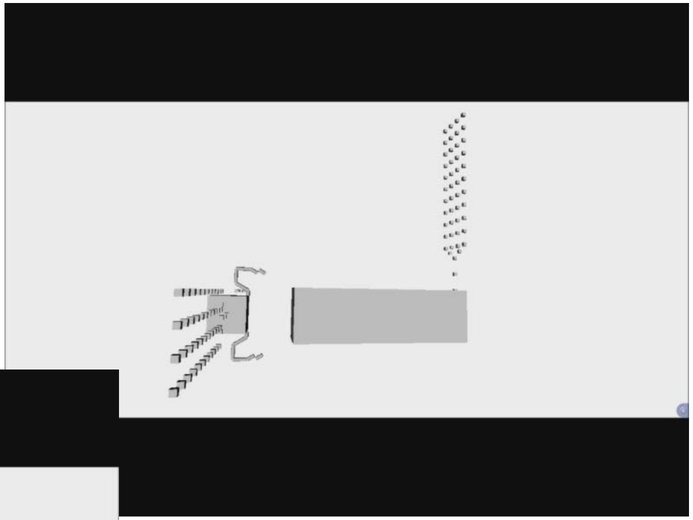

CJTA

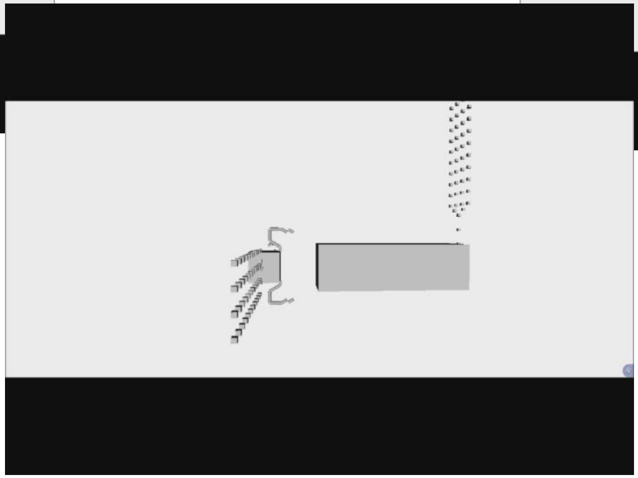

BPFA

Contact maneuver

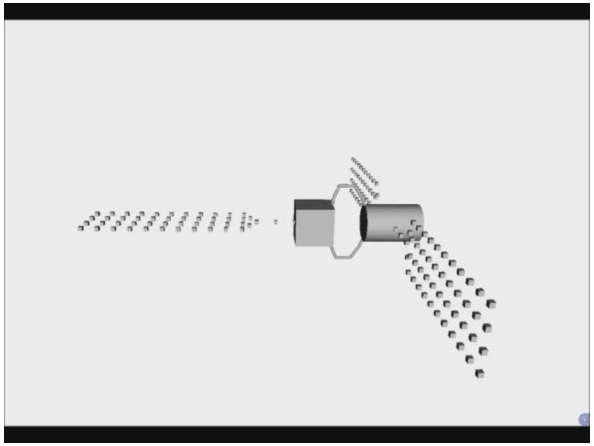

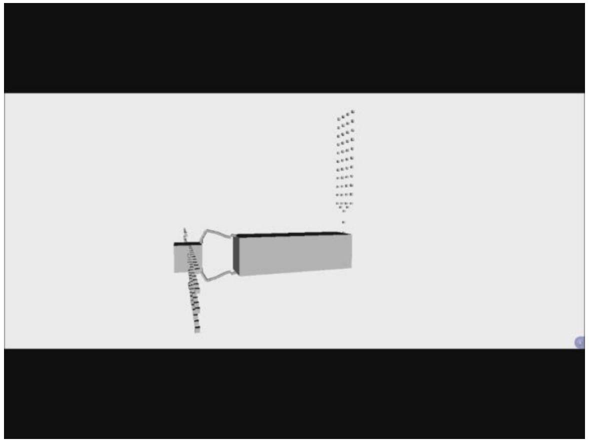

Post-Docking maneuver behaviour

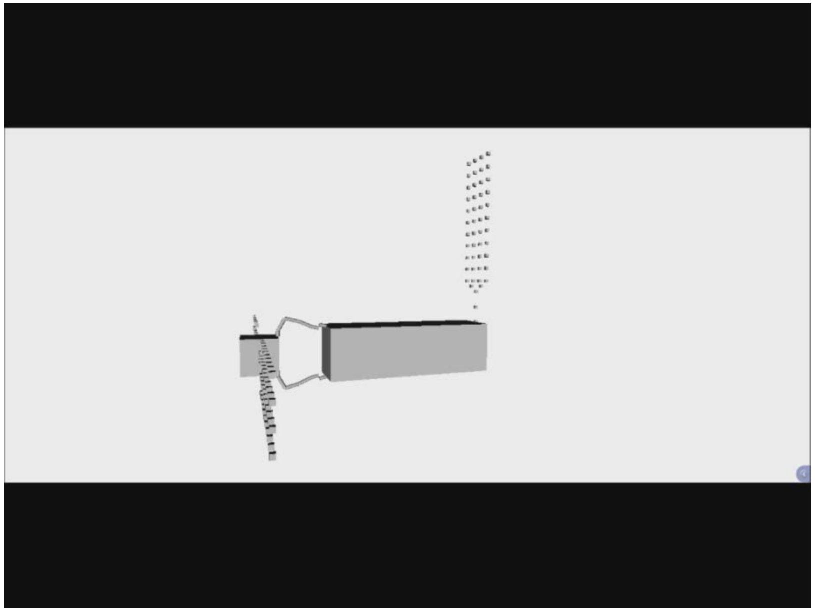

Flexibility Compensation with the Base Platform Control Forces Algorithm (BPCFA)

- Co-simulation schemes: Symulink-MSC. Adams

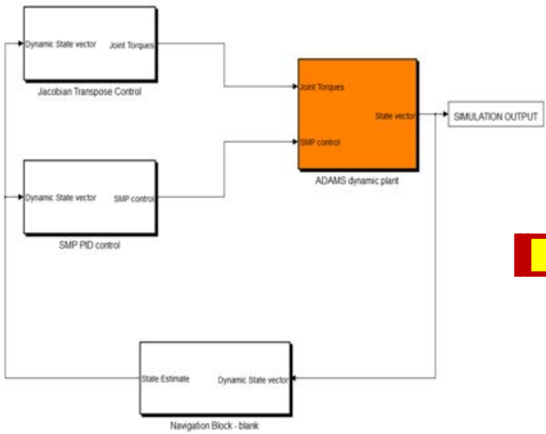

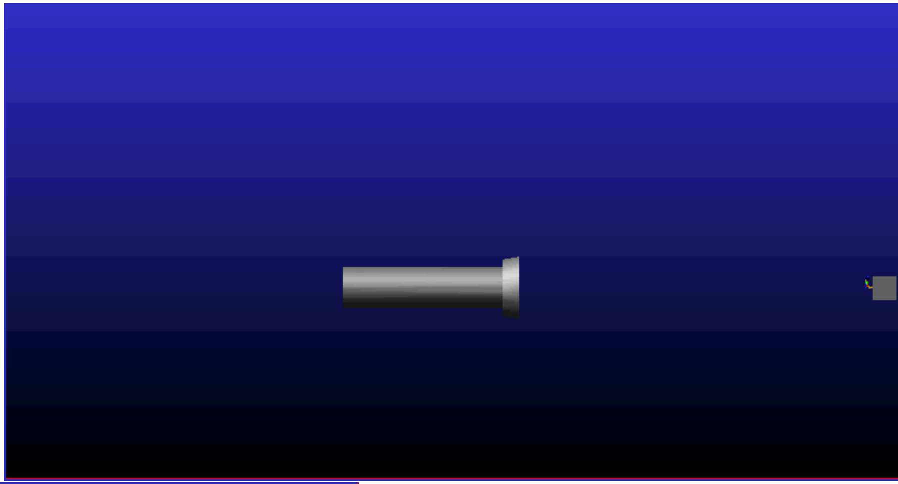

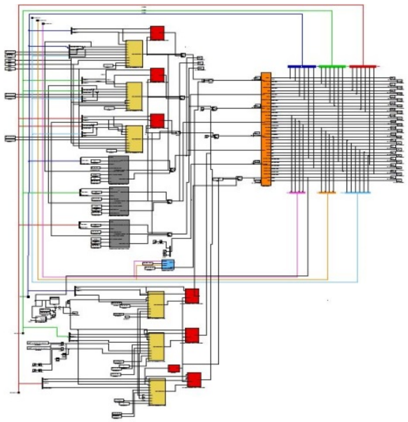

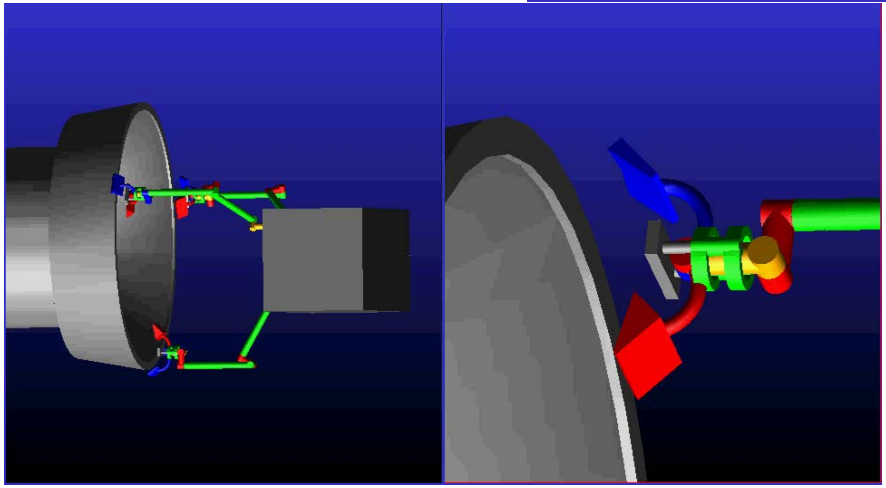

Astrium Researches on Active Debris Removal by Means Robotic Arms

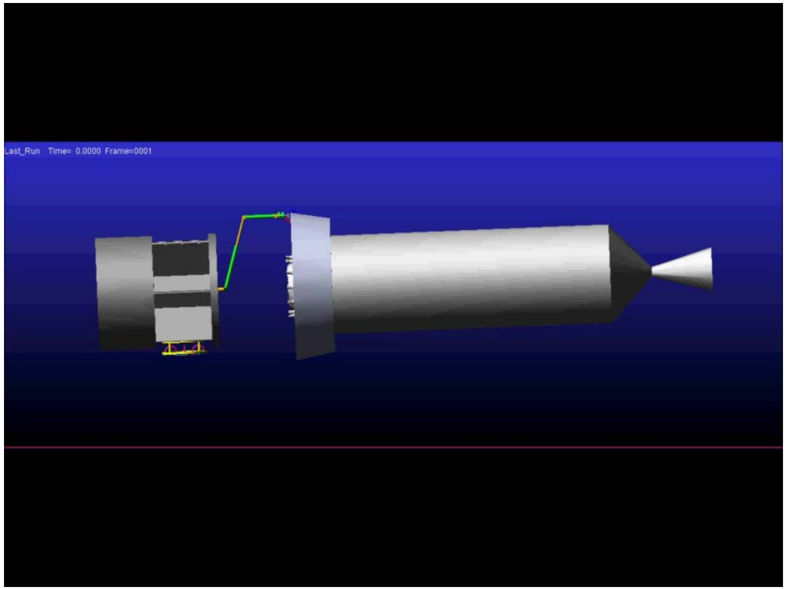

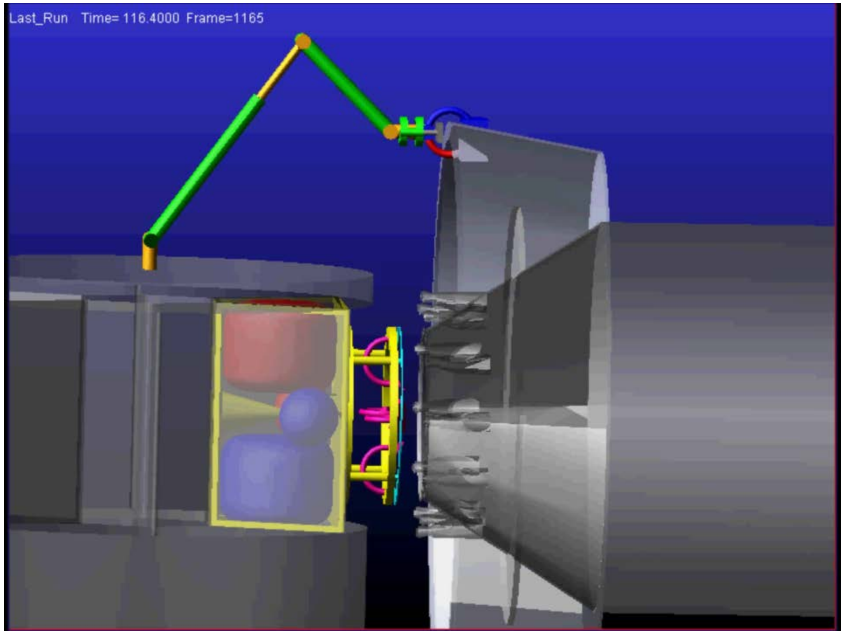

Experimental test-beds: manipulator, end effectors, free-flyer, **rover**

P.Gasbarri

- Flexible Manipulator test-bed
- Different types of End-Effectors
- Free Flyer test-bed
- Rover-test-bed

Studies:

Influence of flexibility on guidance and attitude control

Visual Based techniques for

guidance and control

image analysis

docking approach and (shock) vibration damping

Experimental test-bed: Flexible robotic

P.Gasbarri

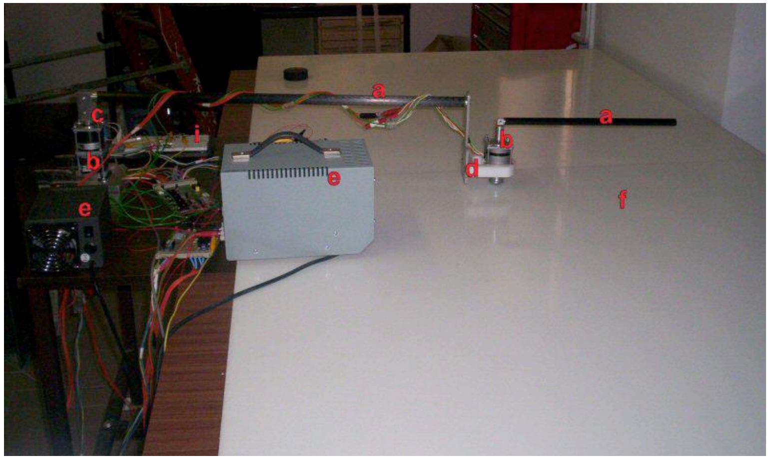

(a) carbon-carbon flexible links
(b) Stepper motors
(c) Gear box
(d) Cart
(e) Power supply
(f) Low friction surface
(g) Driver
(k) Heat sink
(i) Uncoupler

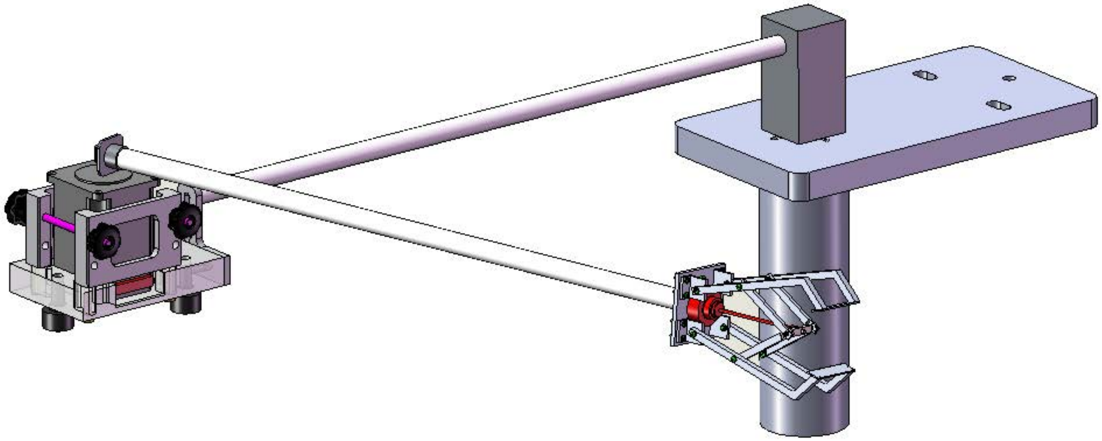

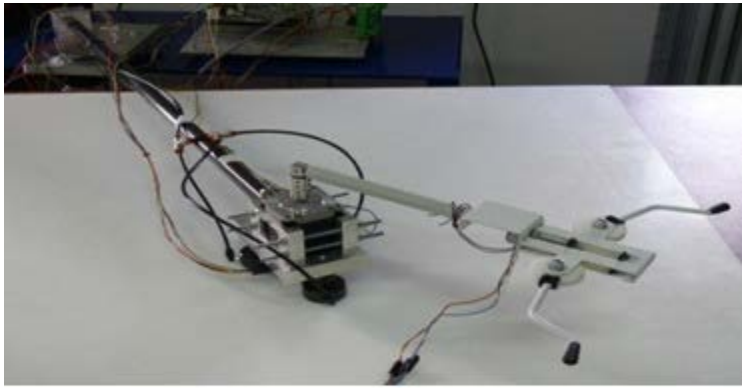

Experimental test-bed: Study of Alghorithms for Visual Based Navigation

P.Gasbarri

Robotic arm for free flyer capture, rendezvous and docking

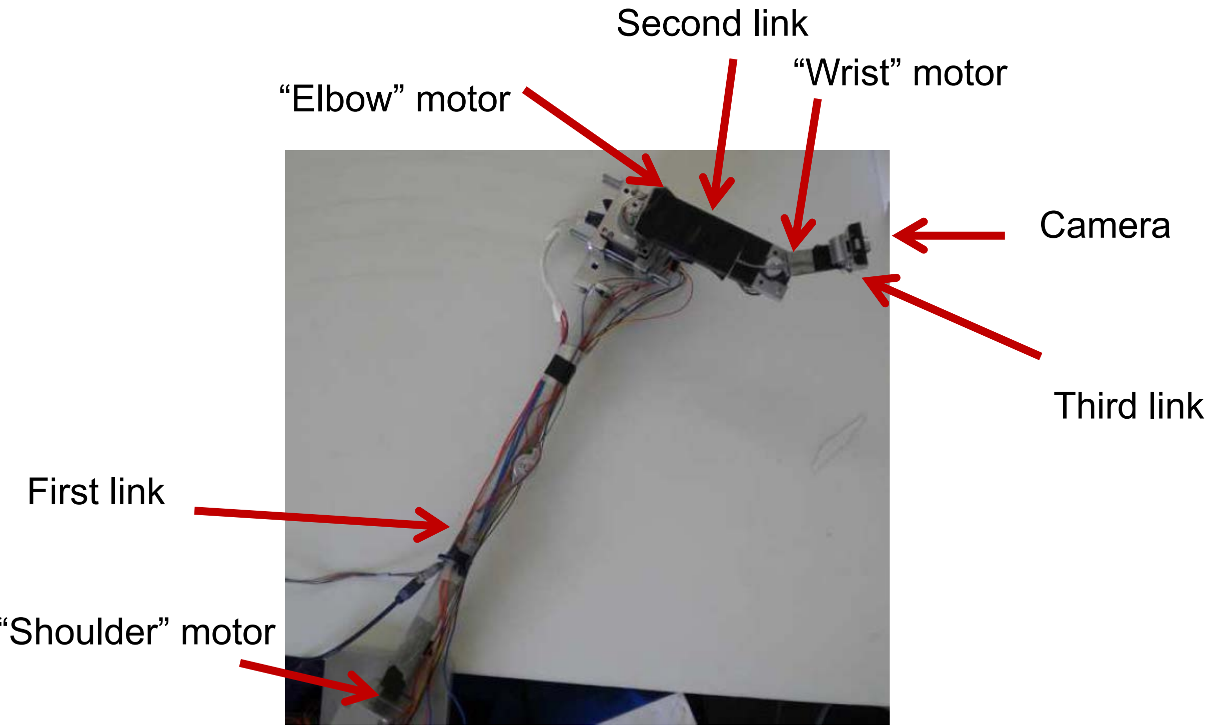

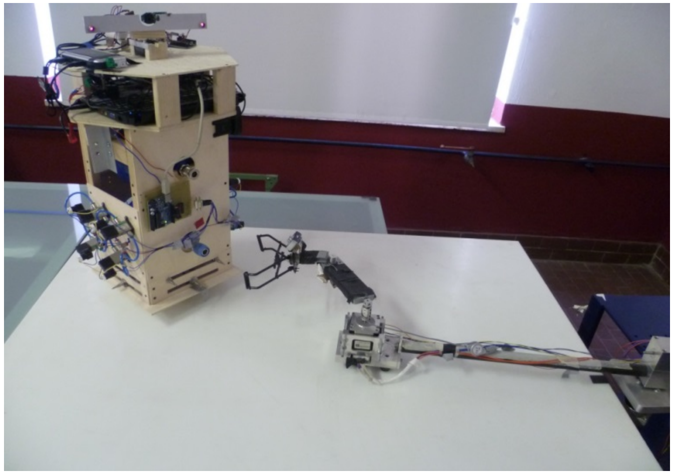

Experimental test-bed: Target Acquisition and Rendezvous

P.Gasbarri

Uncoperative rendezvous and docking

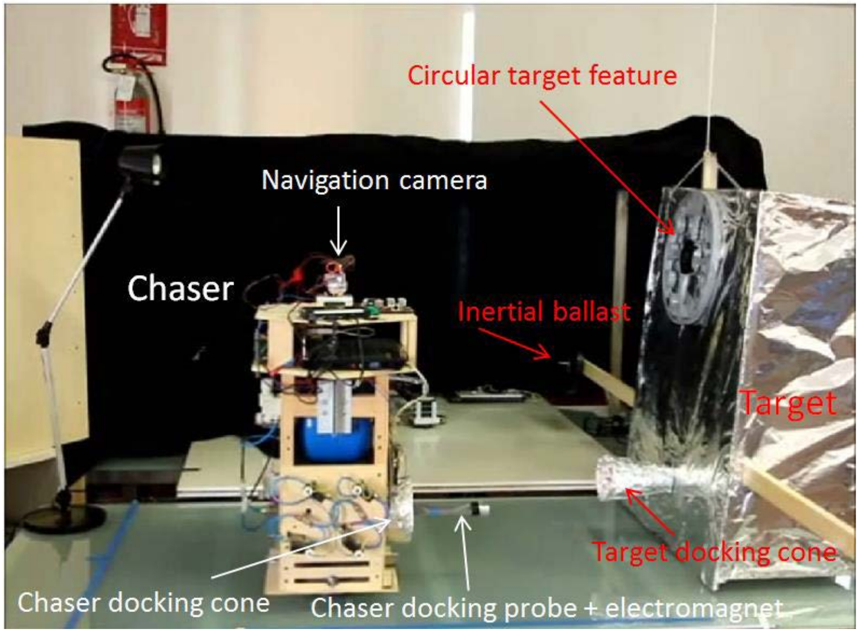

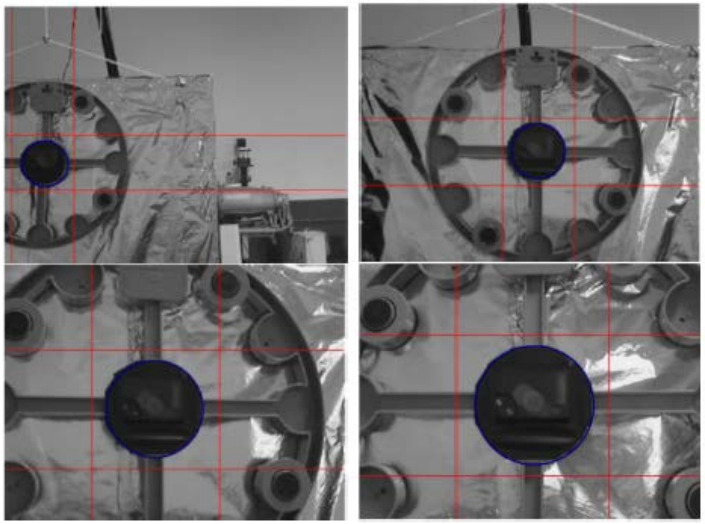

Figure 8 Evolution of the search area (delimited by the red lines) and of the identified circular feature during the docking mission.

Experimental test-bed: Free flying platform

P.Gasbarri

Platform Integrating Navigation and Orbital Control Capabilities Hosting Intelligence Onboard , shortly **PINOCCHIO**

The flyer floats frictionless on a smooth plane, and has **4 degrees of freedom**:
- two translational d.o.f. of the bus
- one rotational d.o.f. of the bus
- one rotational d.o.f. of the camera on top

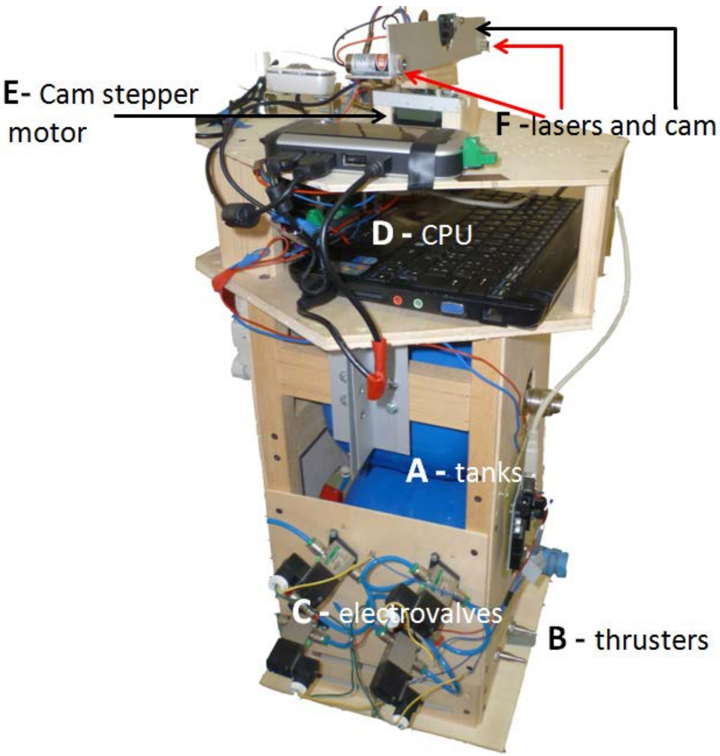

Experiments in flexibility

No delay compensation during attitude maneouver

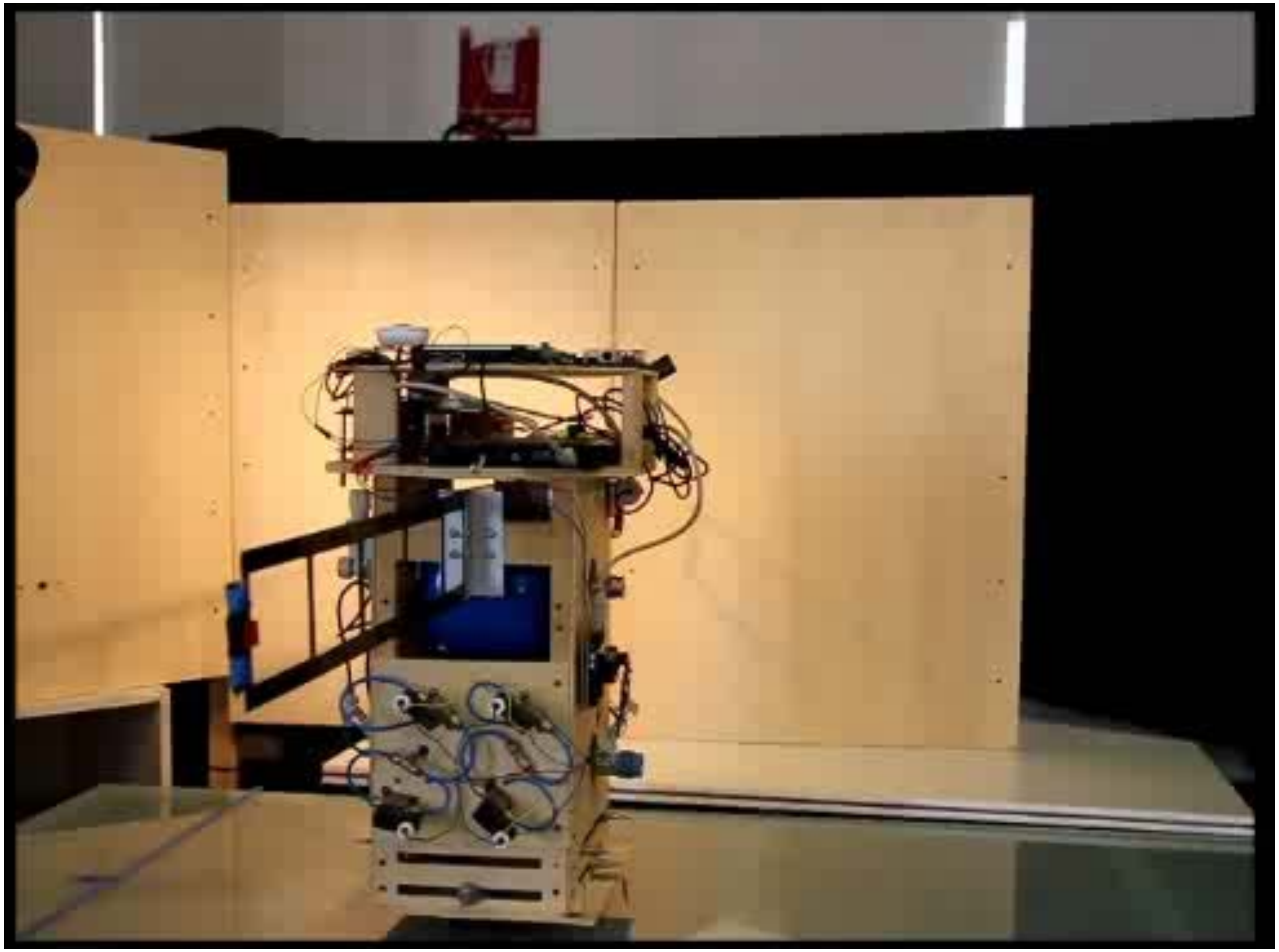

Experiments in flexibility

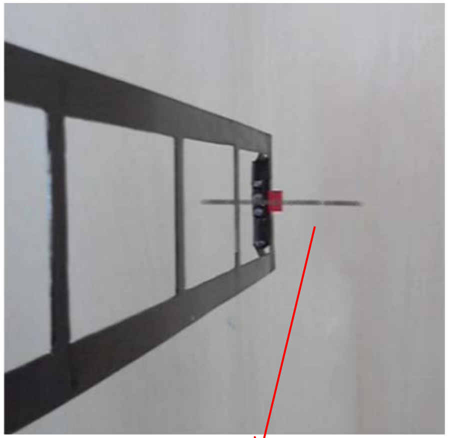

Flexible displacement measurement

Flexible displacements can be included as part of the state of the underactuated system with time control delay

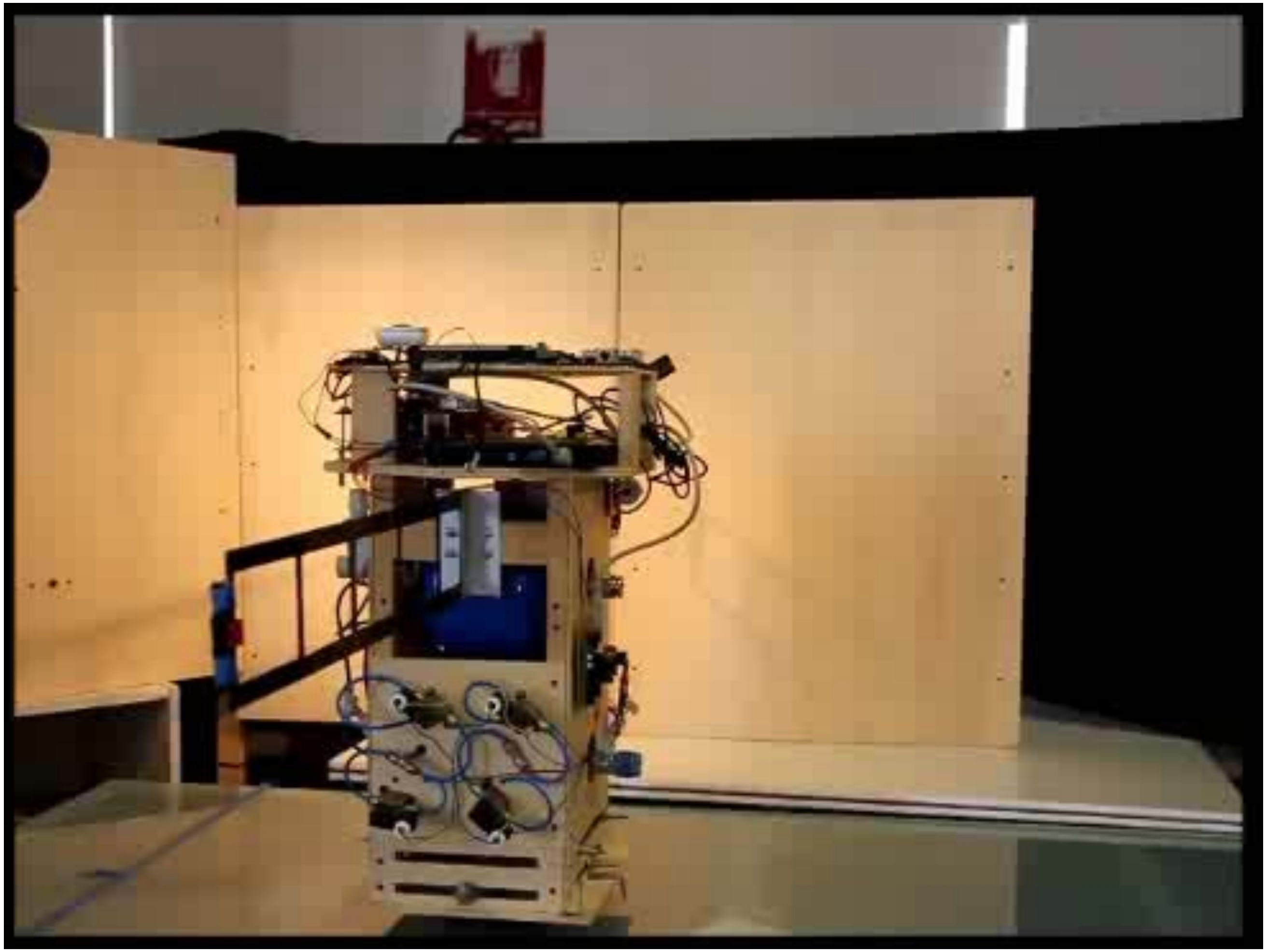

Control shaping techniques **+** Model-based predictor **->** performant system

Experiments on rendezvous and docking

Coordinated Control of a Space Manipulator Tested by means of an Air Bearing Free Floating Platform

P.Gasbarri

Usually, the control of the Chaser's platform (attitude and translation) Is disabled during the mission phases that involve the deployment of the robotic arm and the contact and capture of the target (this is sometimes called a *free-floating* configuration, here labelled **Sequential Control**

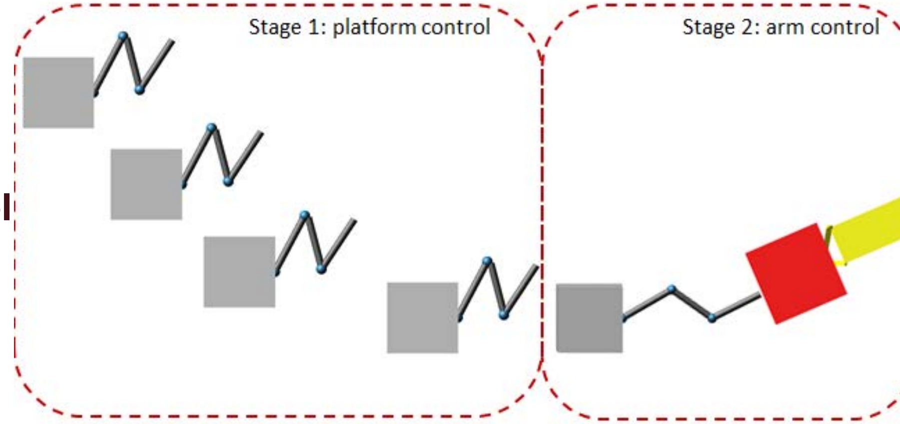

As a different, appealing option, this paper investigates the possibility to use a coordinated control of the platform and of the associated manipulator (sometimes called free-flying configuration, here labelled **Coordinated Control**)

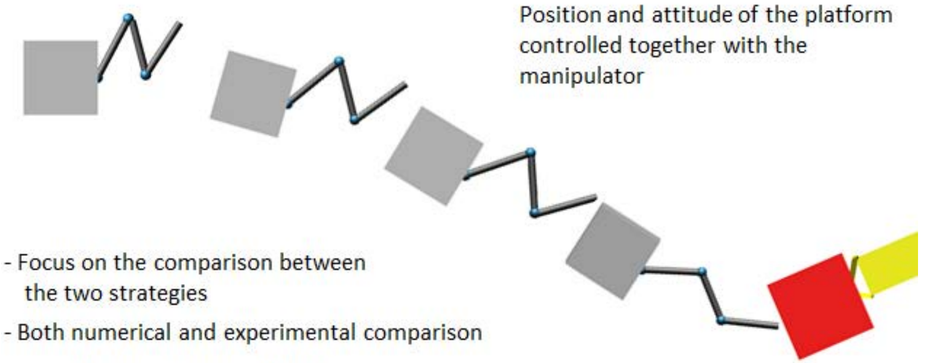

- Focus on the comparison between the two strategies
- Both numerical and experimental comparison
- Topic of current interest (ESA..)

Experimental test-bed: robotic arm

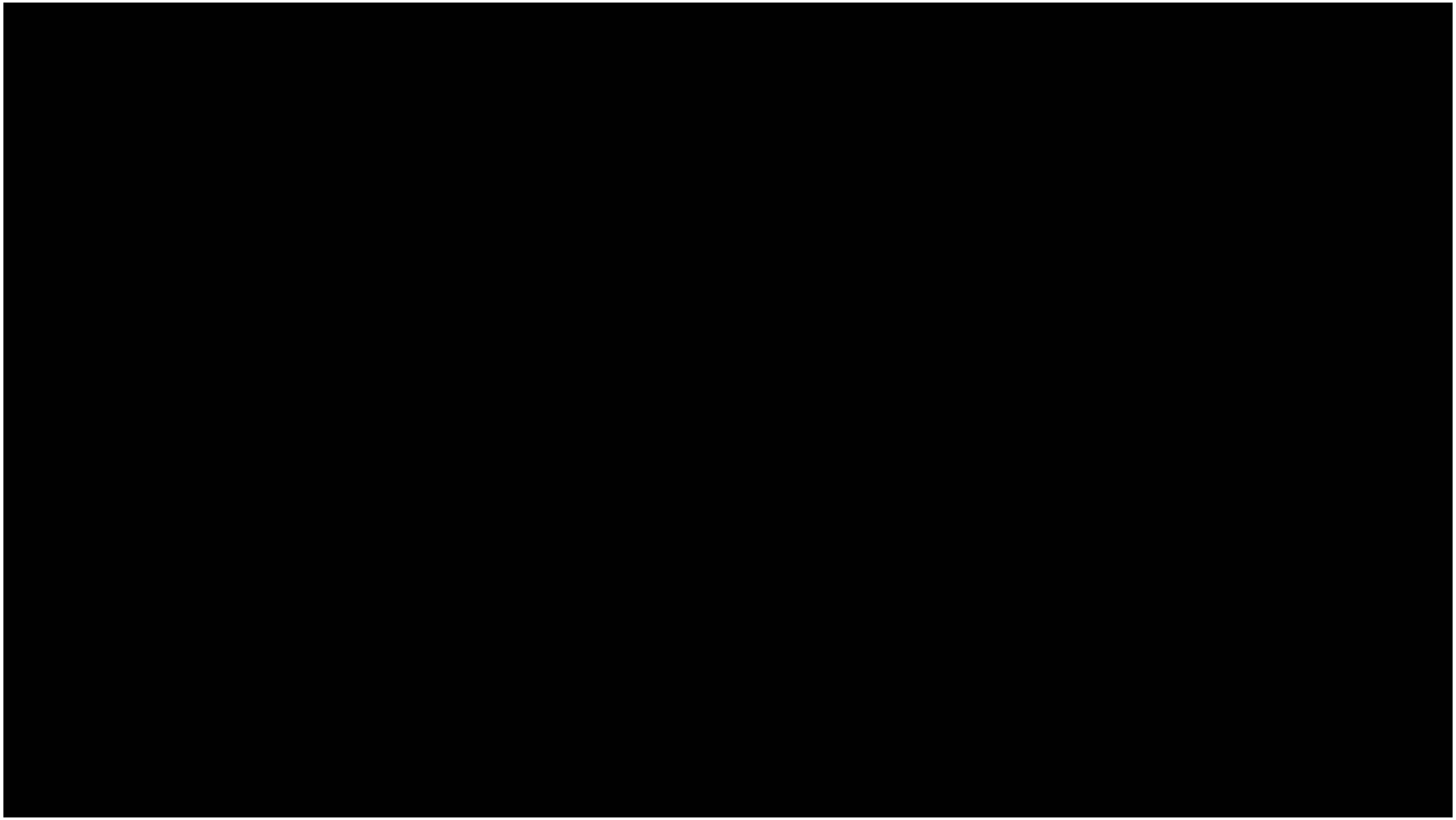

Experimental test-bed: Space rovers

P.Gasbarri

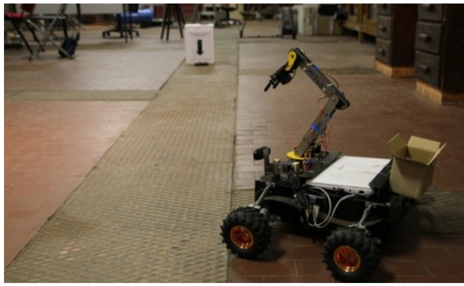

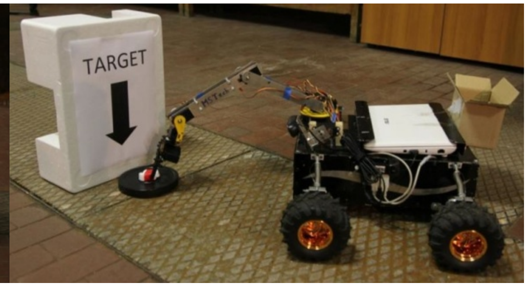

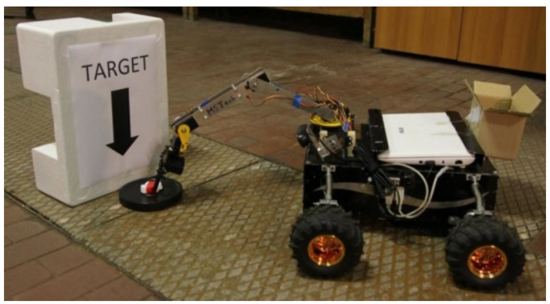

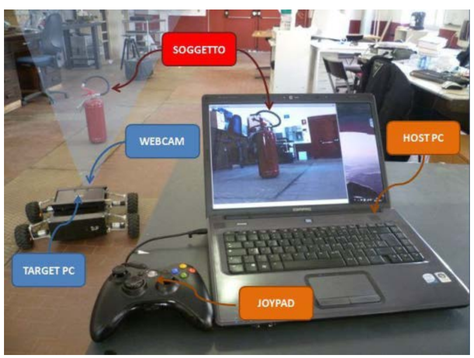

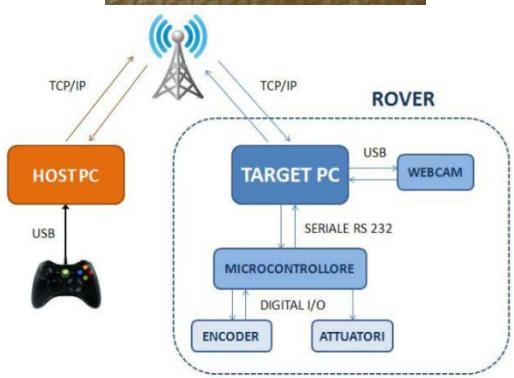

RAGNO (Rover for Autonomous and tele-operated Ground Navigation and Observation)

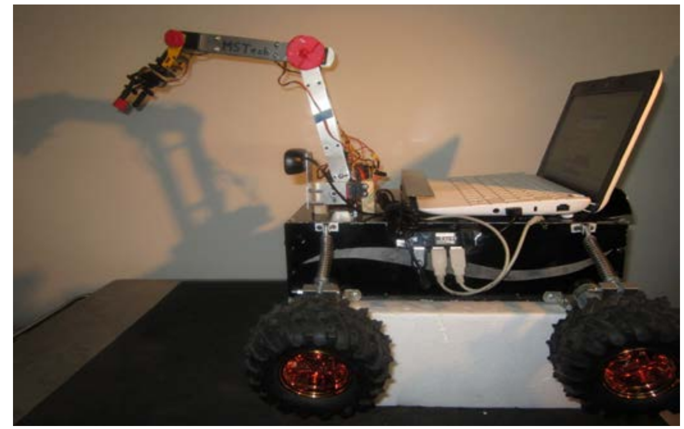

The rover RAGNO on a cradle, showing the robotic arm accommodated on top of the chassis. The laptop (which hosts the joystick console for tele-operation and runs the virtual reality tool to simulate the operation before their execution) has been put close to the rover to indicate RAGNO size. In-house designed suspensions allows RAGNO to overcome 40% steep paths.

Paolo Gasbarri
Pubblicazioni su rivista biennio 2014-2016

1. G.B. Palmerini, P. Gasbarri (in press, on line 6 July 2016), Analysis and Experiments for a System of Two Spacecraft Paired by Means of a Flexible Link, ACTA ASTRONAUTICA (2016), doi:10.1016/j.actaastro.2016.07.004
2. P.Gasbarri, R.Monti (2016), Semi-Analytical Orbital Parameters Description for Thermal Fatigue Analysis, Aerotecnica Missili e Spazio, Vol.96, N.1,pp.32-41, January-February 2016, http://dx.doi.org/10.19249/ams.v95i1.264.g246, http://dx.doi.org/10.19249/ams.v95i1.264
3. P. Gasbarri, M. Sabatini, A. Pisculli, (2016), Dynamic modelling and stability parametric analysis of a flexible spacecraft with fuel slosh, ACTA ASTRONAUTICA, Volume 127, October–November 2016, Pages 141–159, doi:10.1016/j.actaastro.2016.05.018
4. M. Sabatini, P. Gasbarri G.B. Palmerini, (2016), Elastic issues and vibration reduction in a tethered deorbiting mission, Advances in Space Research, Volume 57, Issue 9, 1 May 2016, Pages 1951–1964 doi:10.1016/j.asr.2016.02.010
5. L.Felicetti , P.Gasbarri , A.Pisculli, M.Sabatini, G.B.Palmerini, (2016) Design of robotic manipulators for orbit removal of spent launchers' stages, ACTA ASTRONAUTICA, Volume 119, Feb-Mar.2016, pp.118-130. doi:10.1016/j.actaastro.2015.11.012
6. M. Sabatini, P. Gasbarri G.B. Palmerini, (2015), Delay Compensation For Controlling Flexible Space Multibodies: Dynamic Modeling and Experiments, Control Engineering Practice, Vol.45, Dec. 2015, pp. 147-162. DOI: http://dx.doi.org/10.1016/j.conengprac.2015.09.013
7. A.Pisculli, L.Felicetti, M.Sabatini, P.Gasbarri, G.B.Palmerini, (2015), A Hybrid Formulation for Modelling Multibody Spacecraft, Aerotecnica Missili e Spazio, Vol.94, N.2, 2015, http://dx.doi.org/10.19249/ams.v94i2.126.g113, http://dx.doi.org/10.19249/ams.v94i2.126
8. M. Sabatini, G.B. Palmerini, P. Gasbarri (2015), A testbed for visual based navigation and control during space rendezvous operations, ACTA ASTRONAUTICA, Volume 117, December 2015, Pages 184–196. DOI:10.1016/j.actaastro.2015.07.026
9. P. Gasbarri, A. Pisculli (2015) Dynamic/control interactions between flexible orbiting space-robot during grasping, docking and post-docking maneuvers, ACTA ASTRONAUTICA,Volume 110, May–June 2015, Pages 225-238 DOI:10.1016/j.actaastro.2015.01.024
10. A.Pisculli, P. Gasbarri (2015), A Minimum State Multibody/FEM Approach for Modelling Flexible Orbiting Space Systems, ACTA ASTRONAUTICA, Volume 110, May–June 2015, Pages 324–340 DOI:10.1016/j.actaastro.2014.10.040
11. A.Pisculli , L.Felicetti , P.Gasbarri , G.B.Palmerini, M.Sabatini (2014) A reaction-null/Jacobian transpose control strategy with gravity gradient compensation for on-orbit space manipulators. Aerospace Science and Technology, Vol.38, Pages.30-40, DOI: 10.1016/j.ast.2014.07.012
12. P. Gasbarri, M. Sabatini, N.Leonangeli, G.B. Palmerini (2014) Flexibility Issues in Discrete On-Off Actuated Spacecraft. ACTA ASTRONAUTICA, Vol.101, Pages 81-97,2014, DOI:10.1016/j.actaastro.2014.04.012
13. P. Gasbarri, M.Sabatini, G.B. Palmerini (2014) Ground Tests For Vision Based Determination And Control Of Formation Flying Spacecraft Trajectories. ACTA ASTRONAUTICA, Vol.102, Pp.378-391, DOI:10.1016/j.actaastro.2013.11.035
14. P. Gasbarri, R. Monti, M. Sabatini, (2014) Very Large Space Structures: Non-Linear Control and Robustness to Structural uncertainties. ACTA ASTRONAUTICA Vol. 93, Pages 252-265, DOI: 10.1016/j.actaastro.2013.07.022
15. M.Sabatini, P. Gasbarri, N.Leonangeli, G.B. Palmerini (2014) Analysis And Experiments for Delay Compensation In Attitude Control Of Flexible Spacecraft, ACTA ASTRONAUTICA, Vol. 104, Issue 1, November 2014, Pages 276–292.DOI: doi:10.1016/j.actaastro.2014.08.006

Experimental Modal Analysis

G.Coppotelli, C. Grappasonni

Aim: identification of the dynamic properties of aeronautical/space vehicles in their operative environment – Natural Input Modal Analysis

- Development of theoretical, numerical and experimental methods for the estimate of natural frequencies, damping ratios, and mode shapes from Output-Only data
- Identification of modal parameters from flight tests, support the civil aviation authority in structural verification and flight qualification.
- Developed approach validated and used in both space (launcher structures) and aeronautical (fixed and rotating wings) applications. Application in wind energy engineering also.

Operational Modal Analysis

- ❑ Frequency Domain Decomposition
- ❑ Stochastic Subspace Identification
- ❑ Hilbert Transform Method

$$\tilde{H}_{ii}(\omega) = \sqrt{G_{x_i x_i}(\omega)} e^{j\phi_{ii}(\omega)}$$

$$\tilde{H}_{ij}(\omega) = \frac{G_{x_i x_j}(\omega)}{\tilde{H}_{ii}(\omega)}$$

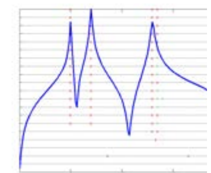

Harmonic Loadings

- ❑ Deterministic component in the excitation loading
- ❑ Rotating structures

Entropy Index

$$H = -\sum_{i=1}^{n} p_i \log(p_i)$$

$$H_{MAX} = H_G = \log\left(\sigma\sqrt{2\pi e}\right)$$

Frequency Response Function

- ❑ Biased FRF from operative responses
- ❑ "*Harmonic-Free*" FRF

$$\tilde{\mathrm{H}}(\omega) = \sum_{n=1}^{M} \left(\frac{\psi^{(\mathrm{n})}\psi^{(\mathrm{n})\mathrm{T}}}{j\omega - \lambda_n} + \frac{\psi^{(\mathrm{n})*}\psi^{(\mathrm{n})\mathrm{H}}}{j\omega - \lambda_n^*} \right)$$

$$\overset{\circ}{\mathrm{H}}(\omega) := \sum_{n=1}^{N_{op}} \left[\frac{\mathrm{R}^{(\mathrm{n})}}{j(\omega - \omega_{opn})} + \frac{\mathrm{R}^{(\mathrm{n})*}}{j\left(\omega - \omega_{opn}^*\right)} \right]$$

$$\overset{\varnothing}{\mathrm{H}}(\omega) = \tilde{\mathrm{H}}(\omega) - \overset{\circ}{\mathrm{H}}(\omega)$$

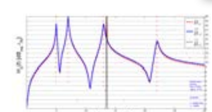

Experimental Modal Analysis

G.Coppotelli, C. Grappasonni

Application cases

VEGA Launcher

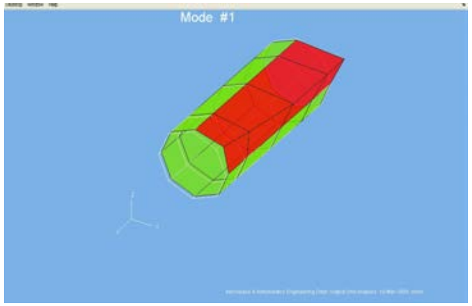

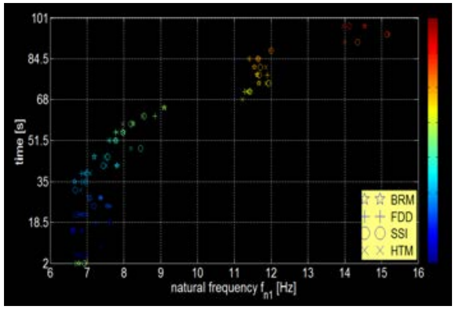

Mode tracking

Westland Helicopter
Lynx

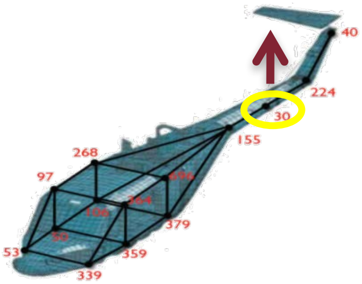

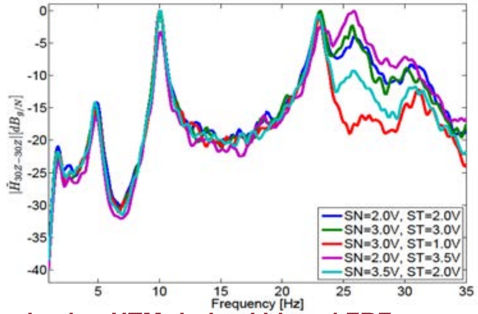

Harmonic removal using HTM-derived biased FRFs

SAVANNAH
Ultra-Light Aircraft

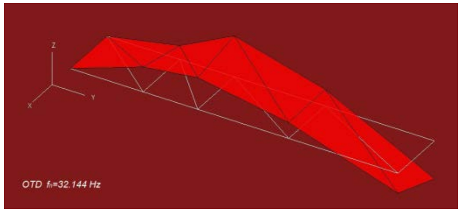

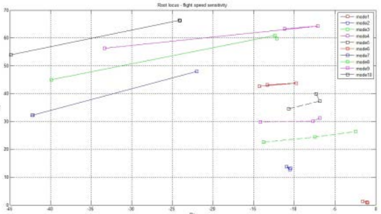

Modal parameters from flight tests: flight speed sensitivity

F.E. Model structural updating

G.Coppotelli, M. Arras

Aim: to develop theoretical/numerical methods for the F.E. model structural updating using dynamic parameters

- Natural frequencies, damping ratios, mode shapes and/or frequency response functions
- Improvements in model identification achieved using FRFs
- Developed approach validated and used in both space and aeronautical applications

$$[M(\{p\})] = \sum_{i=1}^{Nm} p_i^m [M_i^e]$$

$$[K(\{p\})] = \sum_{i=1}^{Nk} p_i^k [K_i^e]$$

From the p-value formulation, model updating is achieved by minimizing a penalty function that reduces the errors between the experimental and numerical models

$$\{\varepsilon\}_{2N_f \times 1} = [S]_{2N_f \times N_p} \{\Delta p\}_{N_p \times 1}$$

$$\{\varepsilon\} = \begin{Bmatrix} 1-\chi_s(\omega_1) \\ \vdots \\ 1-\chi_s(\omega_{N_f}) \\ 1-\chi_a(\omega_1) \\ \vdots \\ 1-\chi_a(\omega_{N_f}) \end{Bmatrix}$$

$$[S] = \begin{bmatrix} \frac{\partial \chi_s(\omega_1)}{\partial p_1} & \cdots & \frac{\partial \chi_s(\omega_1)}{\partial p_{N_p}} \\ \vdots & \cdots & \vdots \\ \frac{\partial \chi_s(\omega_{N_f})}{\partial p_1} & \cdots & \frac{\partial \chi_s(\omega_{N_f})}{\partial p_{N_p}} \\ \frac{\partial \chi_a(\omega_1)}{\partial p_1} & \cdots & \frac{\partial \chi_a(\omega_1)}{\partial p_{N_p}} \\ \vdots & \cdots & \vdots \\ \frac{\partial \chi_a(\omega_{N_f})}{\partial p_1} & \cdots & \frac{\partial \chi_a(\omega_{N_f})}{\partial p_{N_p}} \end{bmatrix}$$

$$\chi_a(\omega_k) \equiv \frac{2\left|\{H^X(\omega_k)\}^H \{H^A(\omega_k)\}\right|}{\{H^X(\omega_k)\}^H \{H^X(\omega_k)\} + \{H^A(\omega_k)\}^H \{H^A(\omega_k)\}}$$

$$\chi_s(\omega_k) \equiv \frac{\left|\{H^X(\omega_k)\}^H \{H^A(\omega_k)\}\right|^2}{\left(\{H^X(\omega_k)\}^H \{H^X(\omega_k)\}\right)\left(\{H^A(\omega_k)\}^H \{H^A(\omega_k)\}\right)}$$

F.E. Model structural updating

G.Coppotelli, M. Arras, E. Conti

Application case: YAK-112 Airworld UAV

- Length: 2.00 [m]
- Weight: 13.7 [Kg]
- Wing span: 2.75 [m]
- Chord: 0.402 [m]

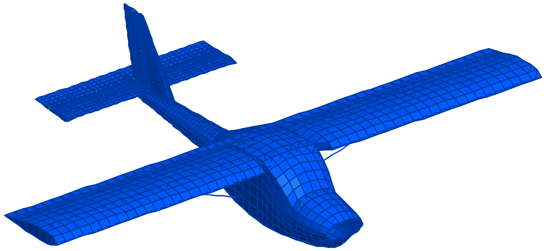

F.E. Model

E.M.A.

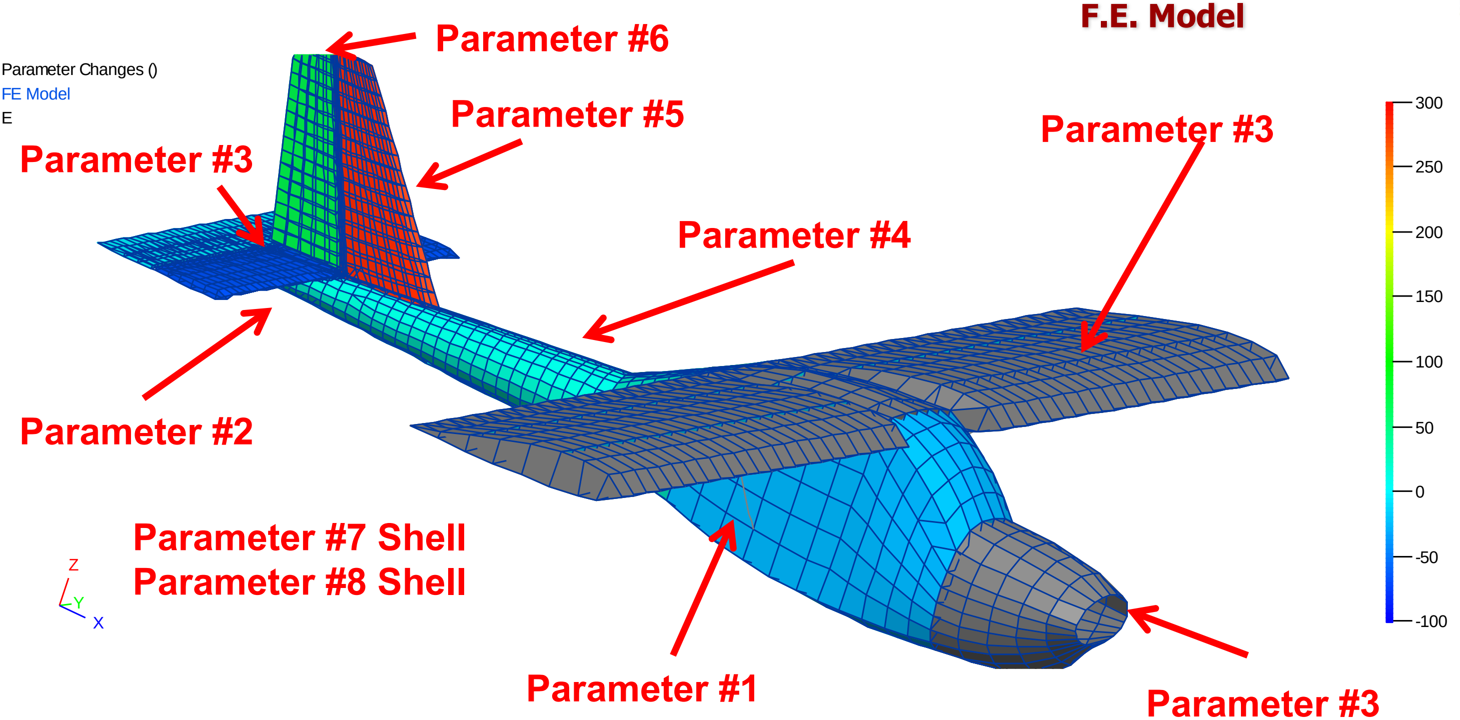

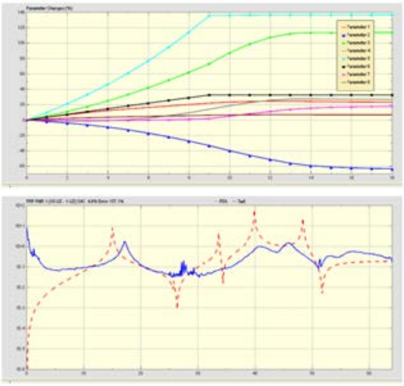

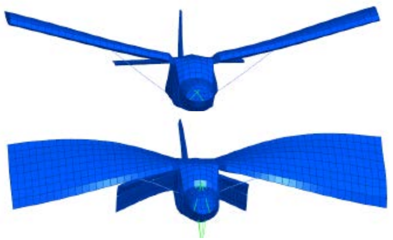

Vibration reduction

G.Coppotelli, V. Camerini

Aim: **to investigate the capability of a vibration suppression approach to reduce the vibration levels aboard a rotary-wing Unmanned Aerial Vehicle, UAV**

- PZT patches passively used as vibration absorbers
- Numerical and experimental investigation of the dynamic properties of a rotorcraft UAV
- Approach validated through flight test campaign.

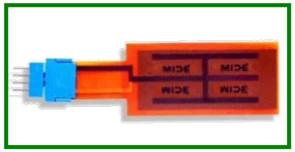

QP10N (ACX)

Optimal shunted PZT electrical parameters:

$$L_{opt} = \frac{1}{C_p^S \left(\omega_n^{OC}\right)^2} \qquad R_{opt} = \frac{\sqrt{2\left[\left(\omega_n^{OC}\right)^2 - \left(\omega_n^{SC}\right)^2\right]}}{C_p^S \left(\omega_n^{OC}\right)^2}$$

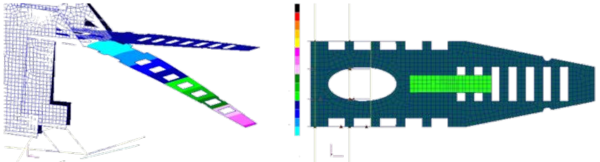

Target mode @ 49.4 Hz ~ 2/rev @ 48.9 Hz

Length	1663 mm
Height	559 mm
Main Rotor diameter	1940 mm
Main Rotor blade	810×94 mm
Tail Rotor diameter	340 mm
Tail Rotor blade	130×36 mm
Operative Empty Weight	8.120 Kg
Payload	11.000 Kg
2-Stroke 52cc Engine	8 Hp
Engine Rotational Speed	3000 - 13000 RPM
1/rev Hover	24.44 Hz

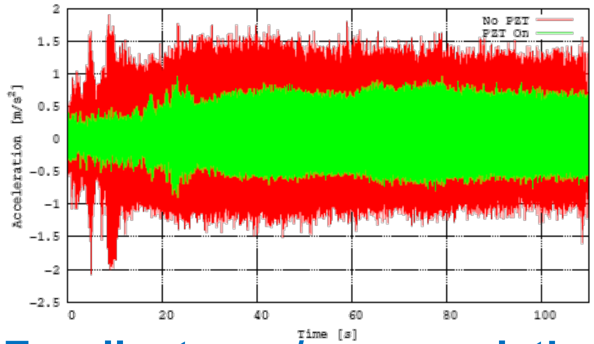

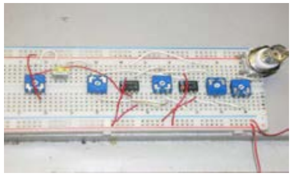

- **Excellent num/exp correlation**
- **50% vibration reduction**
- **0.05% weight increase only**

Health Monitoring using Vibration data

G.Coppotelli, V. Camerini
S. Bendish AIRBUS Helicopters

Aim: Enhance fault detection exploiting the correlation between Condition Indicators

and

Improve trade-off between system false alarms and actual detections

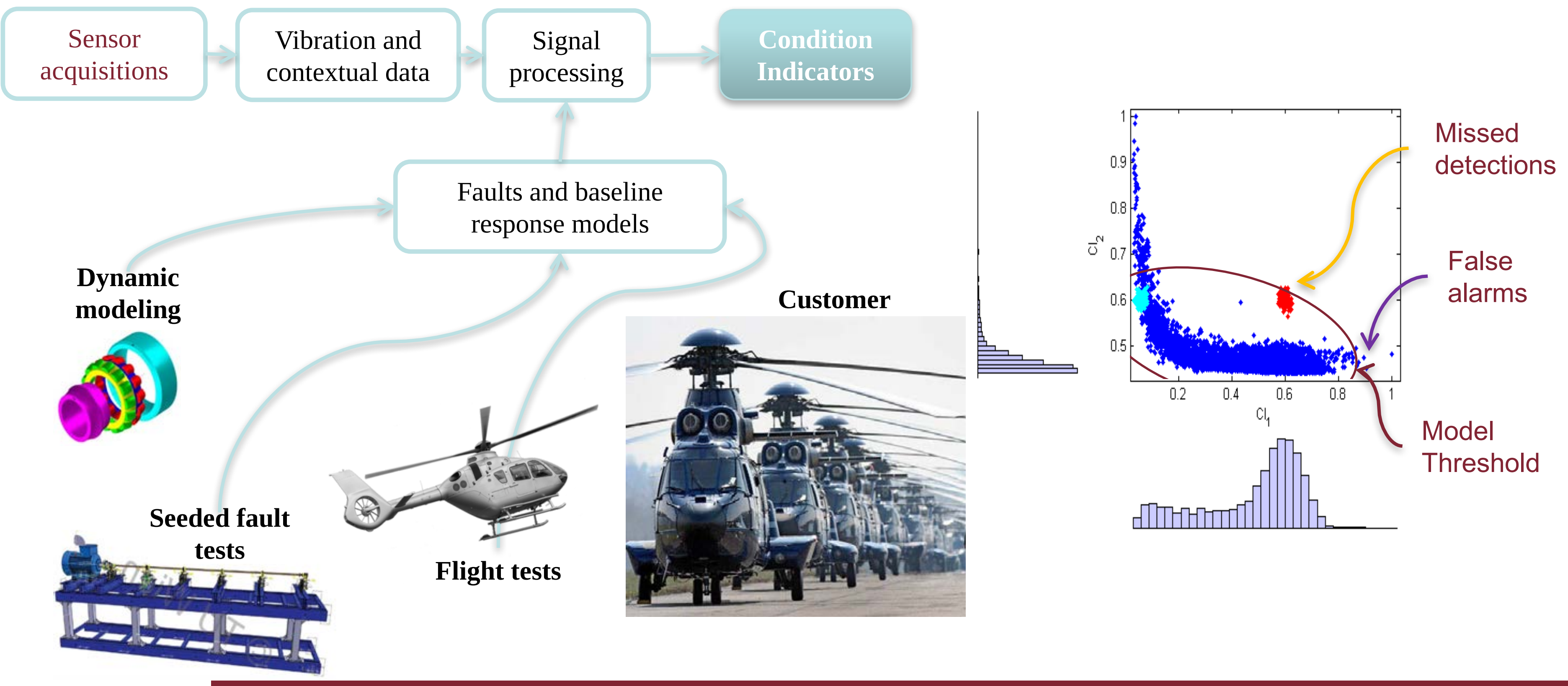

Health Monitoring using Vibration data

G.Coppotelli, V. Camerini

S. Bendish AIRBUS Helicopters

2/2

Experimental case study

Input Drive Shaft gray staining degradation detected from HUMS on servicing H135 (forrmerly EC135)

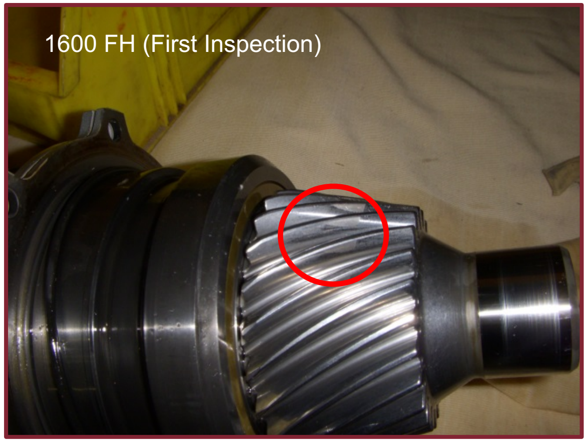

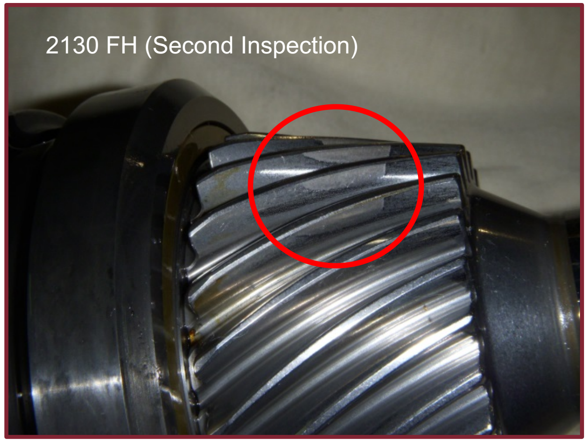

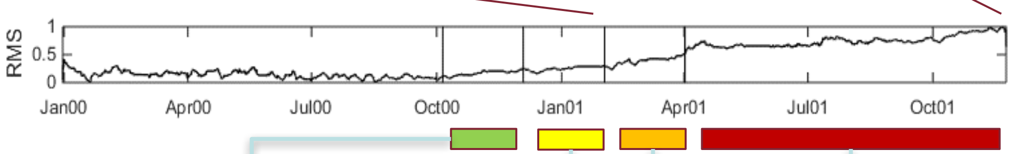

Early degradation

Middle degradat˙

Advanced degradation

>16mm² damaged surface

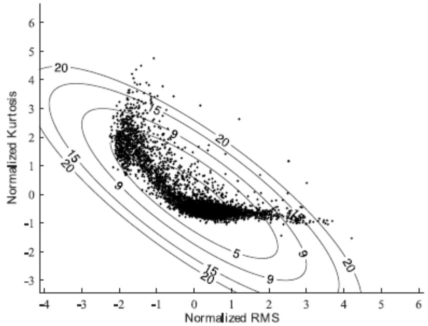

Normalized scatter feature plot and AS Gaussian model contour plot Scatter plot

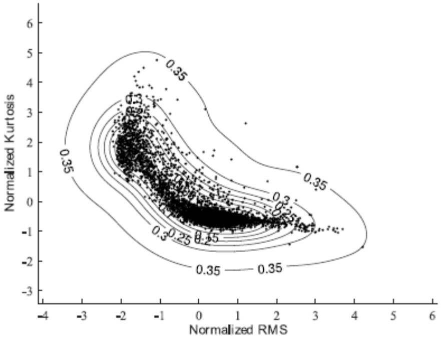

Normalized scatter feature plot and AS SVDD Multivariate Gaussian model contour plot